

Persistence of a reef fish metapopulation via network connectivity: theory and data

Allison G. Dedrick^{a,*1}

Katrina A. Catalano^a

Michelle R. Stuart^a

J. Wilson White^b

Humberto R. Montes, Jr.^c

Malin L. Pinsky^a

a. Department of Ecology, Evolution, and Natural Resources, Rutgers University,
14 College Farm Road, New Brunswick, NJ 08901 USA;

b. Department of Fisheries and Wildlife, Coastal Oregon Marine Experiment Sta-
tion, Oregon State University, Newport, OR 97365 USA;

c. Visayas State University, Pangasugan, Baybay City, 6521 Leyte, Philippines

* Corresponding author; e-mail: adedrick@stanford.edu

1. Current address: Stanford Woods Institute for the Environment, Stanford Uni-
versity, Stanford, CA 94305 USA.

Running title: Empirical metapopulation persistence

Keywords: metapopulation dynamics, self-persistence, network persistence, dispersal kernel, *Amphiprion clarkii*, connectivity (6/10)

Type of article: Letters

Statement of authorship: Conceptualization, Methodology: MLP, JWW, and AGD. Investigation: MLP, MRS, KAC, and AGD. Software, Formal Analysis, Visualization: AGD. Resources: HRM. Data Curation: MRS. Writing - Original Draft: AGD. Writing - Review and Editing: AGD, KAC, MRS, JWW, HRM, MLP. Supervision, Funding Acquisition: MLP.

Data accessibility statement: Sample data, metadata, and analysis code is stored in a GitHub repository and will be made public after acceptance. The repository will be archived with a DOI through Zenodo.

Words in the abstract: 149/150

Words in the main text: 5240

Number of references: 66

Number of main figures, tables, and text boxes: 6

Number of supplementary figures, tables, and text boxes: 19

Acknowledgements

We thank Visayas State University for providing scientific and logistical support during our field sampling in Leyte, Philippines, as well as the municipalities of Bay Bay City and Albuera. We particularly thank Geralde Sucano, Jennifer Hoey, Patrick Flanagan, Joyce Ong, Apollo Lizano, Cecil Bantiles, Rodney Silvado, Beverlito Montalban, Teresita Idara, Rogello Nicanor, Liza Espinosa, Shem San Jose, Noel Alquino, Carlos Balansuna, Froilan Beas, Danilo Marine, Tony Nahacky, and Arturo Bastasa. For financial support, we thank Rutgers School of Environmental and Biological Sciences, NSF #OCE-1430218, an Alfred P. Sloan Research Fellowship, and an ORAU Ralph E. Powe Junior Faculty Enhancement award. This is publication number ## of PISCO, the Partnership for Interdisciplinary Study of Coastal Oceans, funded primarily by the David and Lucile Packard Foundation.

Abstract

Determining metapopulation persistence requires an understanding of both demographic rates and connectivity among patches. Persistence is well understood in theory but has proved challenging to test empirically for marine and other species with high connectivity that precludes classic colonization/extinction dynamics. Here,

we assessed persistence for a metapopulation of yellowtail anemonefish (*Amphiprion clarkii*) using seven years of annual sampling data along 30 km of coastline. We also carefully accounted for uncertainty in demographic rates. Despite stable population sizes through time and sufficient production of surviving offspring for replacement, the spatial pattern of connectivity made the metapopulation unlikely to persist in isolation. To persist, the metapopulation would need higher fecundity or to retain essentially all of the recruits it produced. This assessment of persistence in a marine metapopulation shows that stable abundance alone does not indicate persistence, emphasizing the necessity of assessing both demographic and connectivity processes to understand metapopulation dynamics.

Introduction

The dynamics and persistence of metapopulations depend both on connectivity among patches and on demographic rates within each patch (Hastings and Botsford, 2006; Hanski, 1998). For marine species, connectivity among habitat patches primarily occurs during planktonic larval stages when individuals are hard to track and are able to travel long distances with ocean currents. Because larval connectivity has been perceived to be the greatest uncertainty in these systems, research has centered on quantifying that component (reviewed by White et al., 2019). More recently, it has become apparent that variation in demographic rates among patches is also an uncertain aspect of marine metapopulation dynamics (Hameed et al., 2016; White and Samhouri, 2011). Given both of those uncertainties and driven by both fundamental ecological questions and applied needs (Botsford et al., 2001; White

et al., 2010), a large body of theory has developed to describe how connectivity and local demography interact to determine whether marine metapopulations persist (Burgess et al., 2014; Botsford et al., 2019). Testing this theory, however, has proven substantially more difficult.

For any population to persist, individuals must on average replace themselves during their lifetime. Assessing replacement must account for demographic processes across the life cycle, including how likely individuals are to survive to the next age or stage, their expected fecundity at each stage, the survival to recruitment of any offspring produced, and the distribution of offspring across space (Hastings and Botsford, 2006). A metapopulation can persist via two mechanisms: 1) at least one patch achieves replacement in isolation (self-persistence), or 2) multiple patches receive enough recruitment to achieve replacement through multi-generational loops of connectivity with other patches in the metapopulation (network persistence) (Hastings and Botsford, 2006; Burgess et al., 2014). Theory predicts that habitat patches that are large relative to the mean dispersal distance are likely to be self-persistent (White et al., 2010).

New ways of identifying individuals and determining their origins now allow better measurements of connectivity in marine populations (Almany et al., 2017; D'Aloia et al., 2013). Additionally, a better appreciation of the relevant theory has led to measurement of the demographic factors necessary to assess persistence in field metapopulations (Carson et al., 2011; Hameed et al., 2016; Johnson et al., 2018; Salles et al., 2015). To date, research has suggested that populations on isolated islands can be self-persistent, which might be expected given that they lack nearby

populations from which to receive larvae (Salles et al., 2015). In contrast, small habitat patches spread across a larger reef metapopulation appear to rely on input from surrounding and intervening patches for persistence (Johnson et al., 2018). Isolated habitat patches are rare in the marine environment and clarifying whether intervening habitat patches are sufficient to allow metapopulations to achieve replacement is a key question. Persistence has yet to be quantified in the field for a continuous marine metapopulation.

Here, we further our understanding of metapopulation dynamics in a network of patches along a continuous coastline through a study of yellowtail anemonefish (*Amphiprion clarkii*) in the Philippines. We assessed persistence for all patches of habitat within a metapopulation spread across 30 km of coastline. Based on seven years of data, we found that, despite containing multiple patches with large abundances that were stable over time, the metapopulation was not likely to be persistent without immigration from outside patches.

Methods

Persistence theory and metrics

We considered four primary metrics to assess whether and how the anemonefish metapopulation was persistent: 1) lifetime recruit production (LRP) to assess whether the metapopulation had enough offspring that survived anywhere to achieve replacement, 2) self-persistence (SP) to assess whether any individual patch could persist in isolation without input from other patches, 3) network persistence (λ_c) to assess

whether the metapopulation was persistent as a connected unit, and 4) local replacement (LR) to assess whether a sufficient number of recruits were retained anywhere within the metapopulation to achieve replacement, without explicitly estimating dispersal patterns (Fig. 1a-d). We explain each metric below in detail. To represent the uncertainty in our estimates, we calculated each metric 1000 times, sampling each input parameter from a distribution representing the uncertainty in the empirical estimate (details in Appendix Methods A.9). In our results, we show point estimates of each metric along with uncertainty bounds, defined as the middle 95% of the distribution of values calculated in this Monte Carlo procedure. We provide additional method details, results, tables and figures in the appendix (methods: Appendix A, results: Appendix B, tables: Appendix C, figures: Appendix D).

Lifetime recruit production (LRP)

LRP_i is the expected number of recruits a recruit on patch i will produce in its lifetime,

$$\text{LRP}_i = \text{LEP}_i \times S_e, \quad (1)$$

where LEP_i (lifetime egg production) is the patch-specific number of eggs a recruit produces in its lifetime and S_e (egg-recruit survival) is the fraction of eggs that survive to become recruits (Appendix Fig. D.1).

If $\text{LRP} \geq 1$, individuals produced enough surviving offspring, before considering dispersal, to potentially achieve replacement. If $\text{LRP} < 1$, the population could not

persist without input from outside patches. We considered all recruits produced by adults in our metapopulation to estimate LRP_i , regardless of where they settled.

Self-persistence (SP)

SP_i is the number of offspring a recruit produces that survive to become recruits and settle in the natal patch,

$$\text{SP}_i = \text{LRP}_i \times p_{i,i}, \quad (2)$$

where $p_{i,i}$ is the probability of larval retention on patch i .

A patch i is self-persistent if $\text{SP}_i \geq 1$. If at least one patch is self-persistent, the metapopulation as a whole persists as well (Hastings and Botsford, 2006; Burgess et al., 2014).

Network persistence (λ_c)

Network persistence is the largest real eigenvalue λ_C of the realized connectivity matrix C ,

$$C_{i,j} = \text{LRP}_i \times p_{i,j}, \quad (3)$$

created by multiplying lifetime recruit production (LRP_i) by dispersal probabilities among pairs of patches ($p_{i,j}$) (Burgess et al., 2014). The diagonal entries of C are the self-persistence values for each patch (SP_i).

Network persistence explicitly considers dispersal of individuals among patches

in addition to the reproduction and survival at each patch and requires $\lambda_C \geq 1$ for the network to persist without outside input (Hastings and Botsford, 2006; White et al., 2010; Burgess et al., 2014).

Local replacement (LR)

Local replacement (LR) is the number of recruits a recruit produces in its lifetime that return to settle within the focal metapopulation. LR is related to LRP, but in contrast, LRP also includes recruits that settle outside of the focal metapopulation. LR is defined as

$$LR = LEP_* \times R_e, \quad (4)$$

where LEP_* is lifetime egg production averaged across patches and R_e is the proportion of eggs that survived and returned to recruit at the patches in our focal metapopulation (the 30 km section of coastline). R_e is a modification of egg-recruit survival (S_e) that implicitly considers dispersal in terms of larvae landing inside or outside the metapopulation.

If $LR \geq 1$, enough offspring were locally retained to achieve replacement if they were evenly spread among patches, but the actual dispersal patterns among the metapopulation patches may still prevent replacement if the pattern of multigenerational replacement does not satisfy network persistence (λ_c). LR and λ_c both assess the ability of our patches to persist as an isolated group, but LR treats the network as one large homogenous patch while λ_c explicitly accounts for the structure and

connectivity among patches.

Study species

We focused on a tropical metapopulation of yellowtail anemonefish (*Amphiprion clarkii*, Fig. 2c). Yellowtail anemonefish have a mutualistic relationship with anemones that house small colonies of fish (Buston, 2003b; Fautin et al., 1992). Yellowtail anemonefish are protandrous hermaphrodites and maintain a size-structured hierarchy; within an anemone, the largest fish is the breeding female, the next largest is the breeding male, and any smaller fish are non-breeding juveniles. The fish move up in rank to become breeders only after the larger fish have died. In the tropical patch reef habitat of the Philippines, yellowtail anemonefish primarily spawn from November to May and lay clutches of benthic eggs that the parents protect and tend (Ochi, 1989; Holtswarth et al., 2017). Larvae hatch after about six days and spend 7–10 days in the water column before returning to reef habitat to settle in an anemone (Fautin et al., 1992).

Anemonefish are well-suited to metapopulation studies because dispersal only occurs during the larval phase and adults have limited movement on discrete habitat patches (anemones) (e.g., Buston and D'Aloia, 2013; Salles et al., 2015; Almany et al., 2017). Yellowtail anemonefish tend to behave more like other reef fishes, with wider-ranging territories and stronger swimming abilities (Hattori and Yanagisawa, 1991; Ochi, 1989) than the smaller *A. percula* commonly used in metapopulation studies (e.g., Buston et al., 2011; Salles et al., 2015).

Field data collection

We focused on a set of nineteen reef patches spanning 30 km along the western coast of Leyte island facing the Camotes Sea in the Philippines (Fig. 2a). The habitat patches covered approximately 20% of the sampling region and consisted of rocky patches of coral reef separated by sand flats (Fig. 2a,b). To the north, the patches were isolated from nearby habitat with no substantial reef habitat for at least 20 km, a distance greater than the mean dispersal distance for this species (Pinsky et al., 2010). As such, we considered this to be a relatively isolated metapopulation. Located near a populated coastline, the region experiences anthropogenic effects including fishing, pollution, and runoff from agriculture and a nearby riverbed gravel mine, as well as reef-destroying storms like Haiyan and other typhoons in 2013.

From 2012-2018, we sampled fish and habitat at most patches each year (Appendix Table C.4). Divers using SCUBA and tethered to GPS readers swam the extent of each patch and visited anemones inhabited by yellowtail anemonefish. At each anemone, the divers caught fish 3.5 cm and larger, took a tissue sample, measured fork length, and noted tail color as an indicator of life stage (Moyer, 1976). Starting in 2015, fish 6.0 cm and larger were also tagged with a passive integrated transponder (PIT) tag unless already tagged. Divers also looked for eggs around each anemone and measured and photographed any clutches found. In total, we took fin clips from and genotyped 2406 fish and PIT-tagged 1929 fish across all years and patches combined, marking 3053 individual fish.

Estimating demographic and dispersal parameters from empirical data

Parentage analysis and dispersal kernel

Over seven years of sampling, we genotyped 1729 potential parents and 791 juveniles (some fish fall into both categories in different years) at 1340 single nucleotide polymorphisms (SNPs) and found 71 parent-offspring matches (Catalano et al., in review). We used a distance-based generalized Gaussian dispersal kernel fit from the parent-offspring matches (Catalano et al., in review; Bode et al., 2018), where the relative probability of dispersal p is a function of distance d in kilometers and parameters θ and K_d that control the shape and scale of the kernel (Fig. 3a, Appendix Table C.1, uncertainty details in Appendix Methods A.9). The dispersal kernel estimates the relative dispersal by distance for fish that have survived and recruited, so it does not separately estimate pre-settlement mortality. To find the one-tailed probability of fish dispersing among our patches, we numerically integrated the dispersal kernel using the distance from the middle of the origin patch (i) to the closest (d_1) and farthest (d_2) edges of the destination patch (j), with distances calculated using the `geosphere` package in R (Hijmans, 2017):

$$p_{i,j} = \frac{e^{K_d \theta}}{2\Gamma(\frac{1}{\theta})} \int_{d_1}^{d_2} e^{-(e^{K_d d})^\theta} dd, \quad (5)$$

where Γ indicates the gamma function.

Growth and survival: mark-recapture analyses

Fish marked through genotyping and PIT tags allowed us to estimate growth and survival through mark-recapture. In total, we had 3053 marked fish with size and stage data at each capture.

For growth, we used a von Bertalanffy growth curve:

$$\begin{aligned} L_{t+1} &= L_t + (L_\infty - L_t)[1 - e^{(-k)}] \\ &= e^{(-k)}L_t + L_\infty[1 - e^{(-k)}], \end{aligned} \tag{6}$$

where L_∞ is the asymptotic maximum size across the metapopulation and k is the growth rate. We estimated the parameters from the slope m and y-intercept b_L of the relationship between the length at first capture L_t and the length at a later capture date L_{t+1} for fish recaptured a year later (within 345 to 385 days). The von Bertalanffy parameters are $k = -\ln(m)$ and $L_\infty = b_L(1-m)$ (Hart and Chute, 2009) (Fig. 3b, Appendix Table C.1, uncertainty details in Appendix Methods A.9).

We used the full set of marked fish to estimate annual survival ϕ and probability of recapture p_r using the mark-recapture program MARK implemented in R through the package **RMark** (Laake, 2013). We fit several models with year, size, and patch effects on the probability of survival on a log-odds scale and selected the model with the lowest AIC_c (Fig. 3c, details in Appendix Methods A.3, uncertainty details in Appendix Methods A.9, and full list of models in Appendix Table C.3).

Fecundity

From a regression of eggs per clutch on female size while accounting for egg age (determined by the presence of eyed eggs), we found that fecundity increased with size (Appendix eqn. A.1, see details in Appendix Methods A.4). We only considered reproductive effort for female fish. For sex transition size L_f , we used the average size at which recaptured fish were first observed as female (Fig. 3d, uncertainty details in Appendix Methods A.9).

Lifetime egg production (LEP)

We used an integral projection model (IPM) (Ellner et al., 2016) with size as the continuous structuring trait L to estimate lifetime egg production on each patch i (LEP_i). We initialized the IPM with one recruit-sized individual (recruit defined in Appendix Methods A.1) at the initial annual time step ($t = 0$), then projected forward for 100 years. We used the size- and site-dependent survival (Appendix eqn. B.1) and growth (eqn. 6) functions as the probability density functions in the kernel to project the individual into the next time step, producing a size distribution across time ($v_{L,t}$). We then multiplied by size-dependent fecundity f_L (Appendix eqn. A.1). Integrating across time and size, from a minimum size $L_s = 0$ cm to a maximum $U_s = 15$ cm, gave us the total number of eggs one recruit produced in its lifetime (details in Appendix Methods A.5, uncertainty details in Appendix Methods A.9):

$$\text{LEP} = \int_{t=0}^{\infty} \int_{L=L_s}^{L=U_s} v_{L,t} f_L dL dt. \quad (7)$$

We calculated LEP by patch (LEP_i) and averaged across patches (LEP_*) for a fish of recruit size. We also calculated LEP for a fish of parent size (6.0 cm) averaged across patches (LEP_p), which is used below to estimate egg-recruit survival.

Accounting for density dependence

We would ideally assess persistence when the population is at low abundance and not limited by density dependence; at high density the population growth rate will slow to zero. Density dependence has not been typically addressed in previous metapopulation persistence studies (Johnson et al., 2018; Carson et al., 2011; Hameed et al., 2016), though Salles et al. (2015) considers carrying capacity and available space. Density dependence is particularly clear in anemonefish. Juveniles will prevent others from settling such that each anemone can house only one recently settled anemonefish (Buston, 2003a). This density-dependent mortality reduces the apparent survival of new recruits from our field measurements. We accounted for this effect by scaling up our estimate of recruits (the numerator of eqn. 8, described next) by the proportional increase (D) in unoccupied anemones if all of the anemones occupied by yellowtail anemonefish were unoccupied, where p_A is the proportion of anemones occupied by yellowtail anemonefish and p_U is the proportion of unoccupied anemones: $D = \frac{(p_U + p_A)}{p_U}$. We present results with this density dependence modification in the main text and without the modification in the appendix (with subscript D in Appendix Results B.8, Appendix Figs. D.9, D.10).

Survival from egg to recruit (S_e)

We estimated survival from egg to recruit (S_e) using parentage matches to find the number of surviving recruits produced by genotyped parents (similar to Johnson et al., 2018). However, the number of offspring we assigned back to parents (R_m) is an underestimate of the offspring produced by genotyped parents because it is impossible to sample exhaustively. To account for unsampled offspring, we divided R_m by four factors (described below and with details in Appendix Methods A.8 and Appendix Fig. D.2), in addition to multiplying by D as described above, then divided by the number of eggs produced by genotyped parents:

$$S_e = \frac{\frac{DR_m}{P_h P_c P_d P_s}}{N_g \text{LEPp}}, \quad (8)$$

where N_g was the number of genotyped parents and LEPp was the expected lifetime egg production for a fish that has already survived to parent size p (=6.0cm). P_h was the cumulative proportion of habitat in our patches that we sampled over time, P_c was the probability of capturing a fish if we sampled its anemone, P_d was the proportion of the total dispersal kernel from each of our patches covered by our sampling region, and P_s was the proportion of suitable habitat in our sampling region (details in for each in Appendix Methods A.8, uncertainty of P_c in Appendix Methods A.9).

To estimate the survival and retention of recruits back to our patches (needed for local replacement, LR, eqn. 4), we scaled only by P_h and P_c :

$$R_e = \frac{\frac{DR_m}{P_h P_c}}{N_g \text{LEPP}}. \quad (9)$$

Estimated abundance over time

We examined trends in abundance of breeding females at each patch over time ($F_{i,t}$) to compare to our replacement-based persistence estimates. As with offspring, we scaled up the number of females caught ($F_{c_{i,t}}$) at each patch i in each sampling year t by the proportion of habitat sampled in that patch and year ($P_{h_{i,t}}$) and by the probability of capturing a fish P_c :

$$F_{i,t} = \frac{F_{c_{i,t}}}{P_{h_{i,t}} P_c} \quad (10)$$

We fit a mixed effects model with Poisson errors in which $F_{i,t}$ was the response variable, year was the fixed effect, and there were random effects by patch for both intercept and slope using the package `lme4` in R (Bates et al., 2015).

Exploring alternative geographies and larval navigation

To understand whether results would likely be similar in other geographies, we tested the sensitivity of metapopulation persistence to alternative patch widths and to the proportion of the region that is habitat. We varied the proportion of habitat and the overall width of the region using 19 equally sized and spaced patches. We created connectivity matrices using the new distances between patches and otherwise used the original parameter values and uncertainty sets, using adult survival (ϕ) from the

patch with median survival (the Elementary School patch) for all patches.

We also tested sensitivity to the ability of larvae to navigate to habitat by adding up to a 1 km buffer to the edges of the destination patches when integrating the dispersal kernel and adjusting the scaling parameter P_s (eqn. 8) to account for fewer larvae being lost between patches (details in Appendix Methods A.7).

Results

Demographic rates

From field data, mark-recapture, and parentage analyses, we estimated growth (Fig. 3b, Appendix Results B.3), fecundity (Appendix Table C.1), annual survival (Fig. 3c, Appendix Fig. D.5, Appendix Results B.4), lifetime egg production (Fig. 4a, Appendix Results B.6), egg-recruit survival (Appendix Fig. D.13, Appendix Results B.7), and the dispersal kernel (Fig. 3a, Appendix Results B.2). Details and estimated values are in the Results (Appendix B) and Tables (Appendix C) sections of the appendix. These demographic rates form the basis for assessing whether and how the metapopulation persists.

Persistence metrics

Using our demographic and dispersal results, we estimated average lifetime recruit production (LRP) across patches to be 1.74 [0.93, 5.55] (Fig. 4b, Appendix Fig. D.12). Best estimates of LRP_i at individual patches ranged from 0 to 3.7 (Appendix Table C.5, Appendix Fig. D.8). Averaged across patches, 95% of LRP estimates were

≥ 1 , which means that individuals produced enough offspring to replace themselves. However, LRP does not tell us whether those offspring settled in locations that contributed to persistence.

Considering retention of larvae at individual patches, we did not find any patches with $SP_i \geq 1$ (Fig. 5a), suggesting that no patch could persist in isolation. The Haina patch came closest to self-persistence ($SP_i = 0.088 [0.009, 0.47]$) and had only 0.5% of uncertainty values ≥ 1 , making self-persistence very unlikely.

For network persistence, our estimate of λ_c was 0.20 [0.11, 0.84], with only 1.2% of the estimates of $\lambda_c \geq 1$ (Fig. 5c, Appendix Fig. D.14). Network persistence for this metapopulation was therefore highly unlikely but not impossible. Our estimate of local replacement (LR) was 0.20 [0.11, 0.63], also suggesting lack of independent persistence of this group of patches and very similar to our λ_c estimate. While both LR and λ_c provide information on the ability of our patches to persist as an isolated group, they differ in their assumption of the structure of the population. LR approximates the network of patches as a single well-mixed unit, while λ_c incorporates the spatial structure of the patches and multi-generation dynamics. Results without density dependence compensation also suggested lack of persistence (Appendix Results B.8, Appendix Fig. D.9).

Abundance

Our estimated abundance of females over time had a positive trend for the average patch (slope = 1.08, Fig. 4d), suggesting a slight increase in population size through time. Most individual patches also showed a positive trend in female abundance

through time (Fig. 4d, Appendix Fig. D.7). Therefore, though the metapopulation did not exhibit network persistence, it also did not show signs of decline over the time scale of our study.

Alternative production and geographies

We then examined what conditions would be needed for this metapopulation to reach persistence. With the existing patch configuration and dispersal kernel, the system would need $\text{LRP} \geq 8.4$ (a five-fold increase) to reach network persistence. In turn, this would require a five-fold increase of egg-recruit survival (S_e), of LEP_* , or an equivalent combination of increases across both. If we alternatively considered all arriving recruits as offspring (not just those originating within the metapopulation), LRP would be 11.1, which would be sufficient for persistence. Similarly, our estimate of LR using all recruits arriving to the patches gave an estimate > 1 (2.21), also suggesting there was recruit-recruit replacement for the metapopulation when immigrants were included.

Another route to persistence would be with a different dispersal matrix or habitat density. If dispersal was such that the metapopulation retained all offspring produced, the study region would be persistent because $\text{LRP} > 1$. With the observed dispersal, however, retaining all recruits is difficult to achieve. The coastline had a low fraction of habitat (20%) and would need to be increased to about 85% before enough offspring are retained that the point estimate of $\lambda_c \geq 1$ (Fig. 6a). In contrast, widening the region while maintaining the same habitat density (20%) did not achieve persistence (Fig. 6b) unless habitat density was also increased (Fig. 6c).

As the region widens, the habitat density necessary for persistence decreases, down to 68% habitat at a region 55 km wide. In contrast, allowing for larval navigation had little impact on persistence estimates (Fig. 6d).

Discussion

In this first assessment of demographic persistence of a coastal marine metapopulation, we did not find strong evidence for either self-persistence of an individual patch or network persistence of the entire 30 km area as an isolated region. This inability to persist as an isolated region does not mean that the metapopulation was declining, however. Both population trends and replacement of recruits with immigrants showed that population levels were stable or increasing slightly. Taken together, these metrics suggest that the region required input of immigrants to persist. Despite encompassing a distance substantially larger than mean dispersal, the coastline only persisted as part of a larger metapopulation.

Theory for predicting persistence within patchy habitats has suggested that we expect self-persistence when the mean dispersal distance is small relative to patch size and network persistence in groups of patches when dispersal distances are much larger than patch sizes and where the proportion of habitat in the landscape is about 10-40% (depending on the particular species, population, and maximum reproductive rate, Botsford et al., 2019). Individual patches in the focal metapopulation were too small for self-persistence, but the 30 km region we sampled was about triple the mean dispersal distance of yellowtail anemonefish estimated from previous genetic work (8-9 km, Pinsky et al., 2010; Catalano et al., in review). Rather than a

continuous patch, however, the region was only about 20% habitat. Increasing the proportion of habitat, however, suggested that even 40% habitat coverage would not be sufficient to achieve persistence and this metapopulation would require almost continuous habitat to persist. Similar to fish on small patches in the Caribbean (Johnson et al., 2018), this anemonefish metapopulation depends on the production and connectivity of outside patches. One possible path to persistence would be through nearby patches with higher egg production or survival. In such a case, even a small increase in area could create a persistent network. Deeper reefs, for example, are often healthier than shallower reefs (Cinner et al., 2016). In this system, offshore reefs, with higher coral cover and less silt, could have higher anemonefish survival and contribute disproportionately to regional metapopulation persistence.

Our finding of a lack of isolated persistence differs markedly from persistence findings of other reef fish metapopulations. On reefs surrounding Kimbe Island, Salles et al. (2015) report self-persistence of individual anemonefish subpopulations in lagoons that were of similar size (approximately 100-500 m long) to our individual patches, as well as network persistence of the 800 m wide metapopulation around the island. This persistence finding is at a dramatically smaller scale than for our focal metapopulation in the Philippines. Additionally, Johnson et al. (2018) estimated that four reefs of a combined area of only 2.6 km^2 (four 65 ha patches) would be sufficient for network persistence of a damselfish metapopulation across multiple islands in the Bahamas. This area is roughly equivalent to a 26 km coastline section, which is shorter than our sampling region. To persist, these two offshore metapopulations either had much higher retention of recruits or higher recruit production than did

our coastline patches.

Though lack of sufficient connectivity and retention is thought to inhibit network persistence in some systems (e.g., insufficient retention of offspring within reserves for eastern oysters (*Crassostrea virginica*) in North Carolina; Puckett and Eggleston, 2016), low production of surviving recruits seems the likelier explanation in the Philippines. Recruit production was much lower in the Philippines than in the Kimbe Island populations, where Salles et al. (2020) estimated that an average individual produced 0.54 offspring over two years that recruited back to the natal population, more than twice our estimate of lifetime local replacement ($LR = 0.20$). Lower production at our patches could be due to lower egg production, slower growth, or lower adult survival, all likely affected by habitat quality (e.g. Salles et al., 2020; Hayashi et al., 2019). Our study system was near a populated coastline and experienced anthropogenic effects, including pollution and silt, that can reduce demographic rates. Adult survival, for example, was lower at the two patches just downstream of a gravel mine (N. and S. Magbangon). Even at our higher-survival patches (38% annual survival for a 6 cm fish and 53% for a 10 cm fish at Tomakin Dako, for example), survival was lower than estimates from the populations at Kimbe Island (85% annual survival, Salles et al., 2015). Estimates of annual survival in other reef fish species are closer to the lower survival we found for yellowtail anemonefish than the higher survival of *A. percula* at Kimbe Island (approximately 30% annual survival for bluehead wrasse (*Thalassoma bifasciatum*) and bicolour damselfish (*Stegastes partitus*), respectively; Warner and Hughes, 1988; Figueira et al., 2008). Metapopulation growth rates in other reef fish (e.g., Figueira, 2009) and marine species more broadly (Carson et al.,

2011) are highly sensitive to adult survival and other demographic parameters.

Temporal variability in demographic or dispersal parameters on a time scale longer than our sampling might also enable persistence of our patches in isolation (similar to the storage effect, Warner and Chesson, 1985) rather than as part of a larger metapopulation. Successful recruitment events on the decadal scale, for example, sustain rockfish populations on the west coast of the United States through the intervening weak recruitment years (e.g. Tolimieri and Levin, 2005). Our study could have missed a particularly strong recruitment event driven by variable ocean connectivity (simulations suggest that 20 years are necessary to capture the full extent of ocean variability in the Coral Triangle region surrounding our patches; Thompson et al., 2018). Strong recruitment would need to occur at least once a generation to maintain patch populations without switching to colonization and extinction dynamics, however, which we do not see. Our study likely spans the generation time of a yellowtail anemonefish (roughly 5 years) so variable strong recruitment, while possible, is unlikely to sustain our populations.

Understanding marine population persistence in the context of broader metapopulation theory requires reconciling replacement-based persistence analysis with classic colonization-extinction and source-sink dynamics (Sale et al., 2006). At the patch level, many marine metapopulations do not exhibit the colonization-extinction dynamics (or do only on a decades to centuries timescale, Smedbol et al., 2002) that underpin our understanding of many terrestrial metapopulations (e.g, Hanski, 1998; Moilanen et al., 1998). Marine metapopulations more often instead consist of continuously-occupied patches connected by dispersal (Kritzer and Sale, 2006). Be-

cause dispersal is so widespread, patches in marine systems are not easily classified as sources or sinks in the classical fashion (Figueira and Crowder, 2006; White and Samhouri, 2011). For example, despite being unable to persist in isolation, our region is not technically a sink (Pulliam, 1988) because $LRP > 1$. For metapopulations, lack of self-persistence can have two causes: reproduction does not balance mortality losses within a patch (a sink) or sufficient recruits are produced but not retained (as we found in the Philippines). Metapopulations likely lie on a continuum between extinction-colonization dynamics and exchange among populated patches (Kritzer and Sale, 2006) but the latter many be a more practical approach to characterizing dynamics for metapopulations in which exchange is frequent relative to organisms' generations times (Hastings and Botsford, 2006).

In this system and others, density dependence presents a sampling challenge. Persistence criteria (Hastings and Botsford, 2006; Burgess et al., 2014) ask whether a population at low abundance can grow and recover rather than going extinct. In real populations, however, it can be challenging to estimate density-independent demographic rates because density dependence is occurring in the population as it is sampled during dispersal (Nowicki and Vrabec, 2011) and reproduction (Rodenhouse et al., 2003). In anemonefish, density dependence is likely most important immediately post-settlement, as it is for many species, including corals, trees, and butterflies (Vermeij and Sandin, 2008; Harms et al., 2000; Nowicki et al., 2009). However, density dependence could continue to be important throughout life due to social hierarchies in anemonefish colonies (Buston and Elith, 2011). Our calculations of persistence in this paper did not account for longer term post-settlement density

dependence, which would be an interesting area of further research.

Understanding persistence is critical for the management of spatial populations, such as siting marine protected areas (Kaplan et al., 2009), assessing habitat fragmentation risks (Smith and Hellmann, 2002; Fahrig, 2001) and conserving species in the face of climate change (Coleman et al., 2017; Fuller et al., 2015). Though models and theory provide us with expectations, we are only beginning to tackle these questions empirically. While rules of thumb have been widely used in marine ecology and conservation, they may be far from accurate for many study systems. Fortunately, tools now exist to permit a more precise evaluation of demographic rates that can enable assessment of persistence — or lack thereof. Spatial scales of metapopulation persistence in marine systems are likely to be large, despite evidence that dispersal distances are shorter than previously expected (Jones et al., 1999; Almany et al., 2007). Importantly, persistence of coastal metapopulations may rely on high quality habitat refugia to a greater extent than has been widely recognized.

Figures

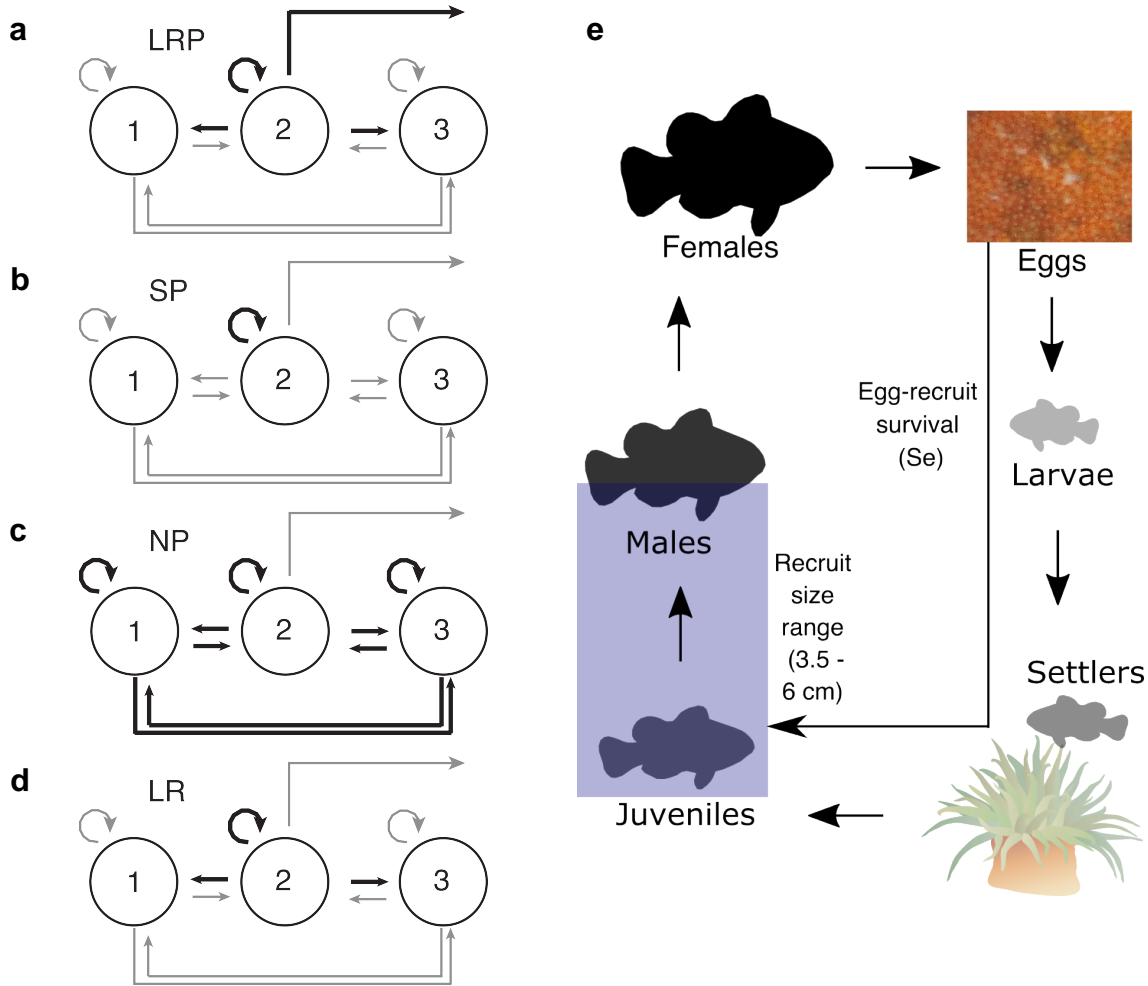


Figure 1: Schematics of the persistence metrics (a-d): a) lifetime recruit production (LRP, eqn. 1), b) self-persistence (SP, eqn. 2), c) network persistence (λ_c , first eigenvalue of eqn. 3), and d) local replacement (LR, eqn. 4). Black lines indicate the demographic processes considered by each persistence metric. e) The life cycle of yellowtail anemonefish, including the range of sizes considered to be recruits (recruit definition in Appendix Methods A.1).

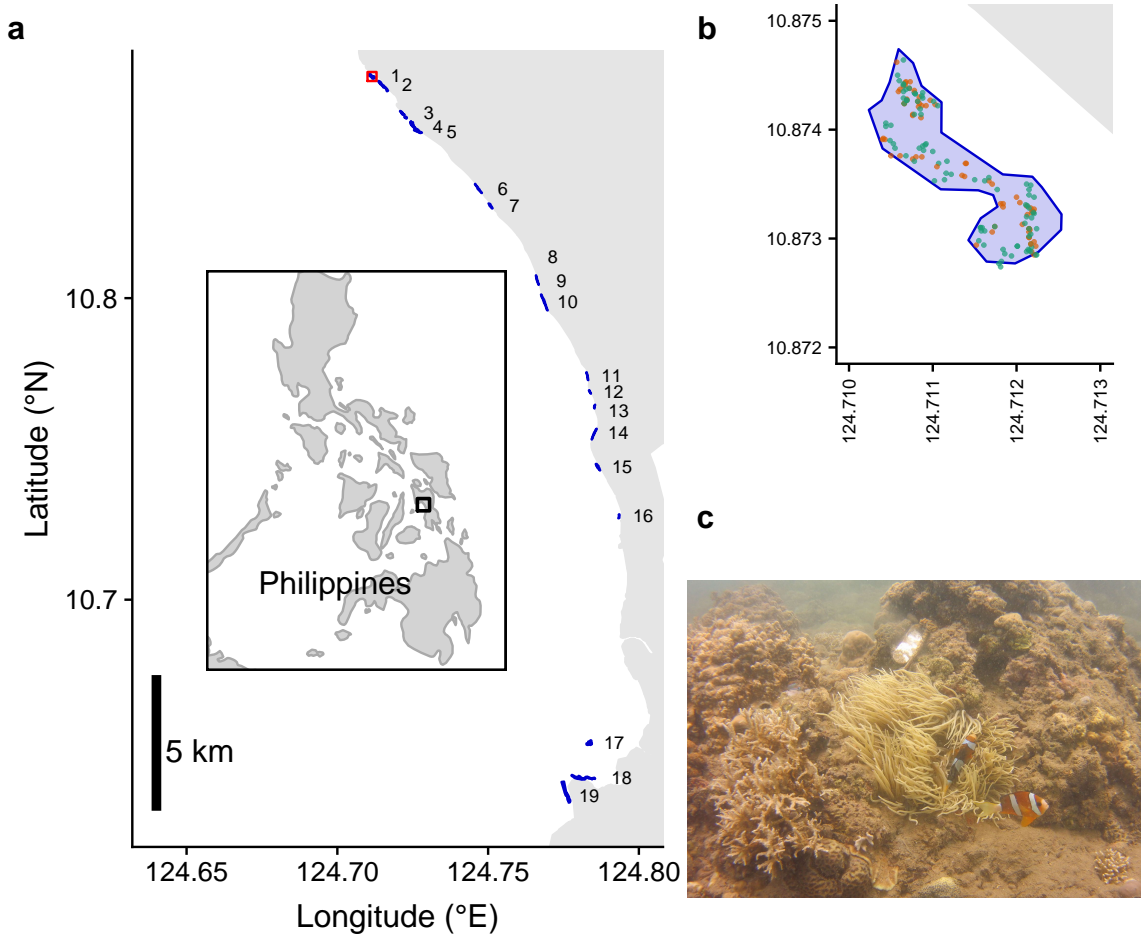


Figure 2: a) Map of the patches along the coast of Leyte in the Philippines. From north to south, the patches are: 1) Palanas, 2) Wangag, 3) North Magbangon, 4) South Magbangon, 5) Cabatoan, 6) Caridad Cemetery, 7) Caridad Proper, 8) Hicgop South, 9) Sitio Tugas, 10) Elementary School, 11) Sitio Lonas, 12) San Agustin, 13) Poroc San Flower, 14) Poroc Rose, 15) Visca, 16) Gabas, 17) Tomakin Dako, 18) Haina, and 19) Sitio Baybayon. b) Zoomed-in map of the northern-most patch, Palanas (red box on map), to show anemone arrangement. Anemones are colored as occupied by yellowtail anemonefish (green) or unoccupied by anemonefish (orange), using colors generated with Brewer (2020). c) An example anemone occupied by yellowtail anemonefish in a typical habitat. The metal anemone tag is visible just above the anemone on the rock.

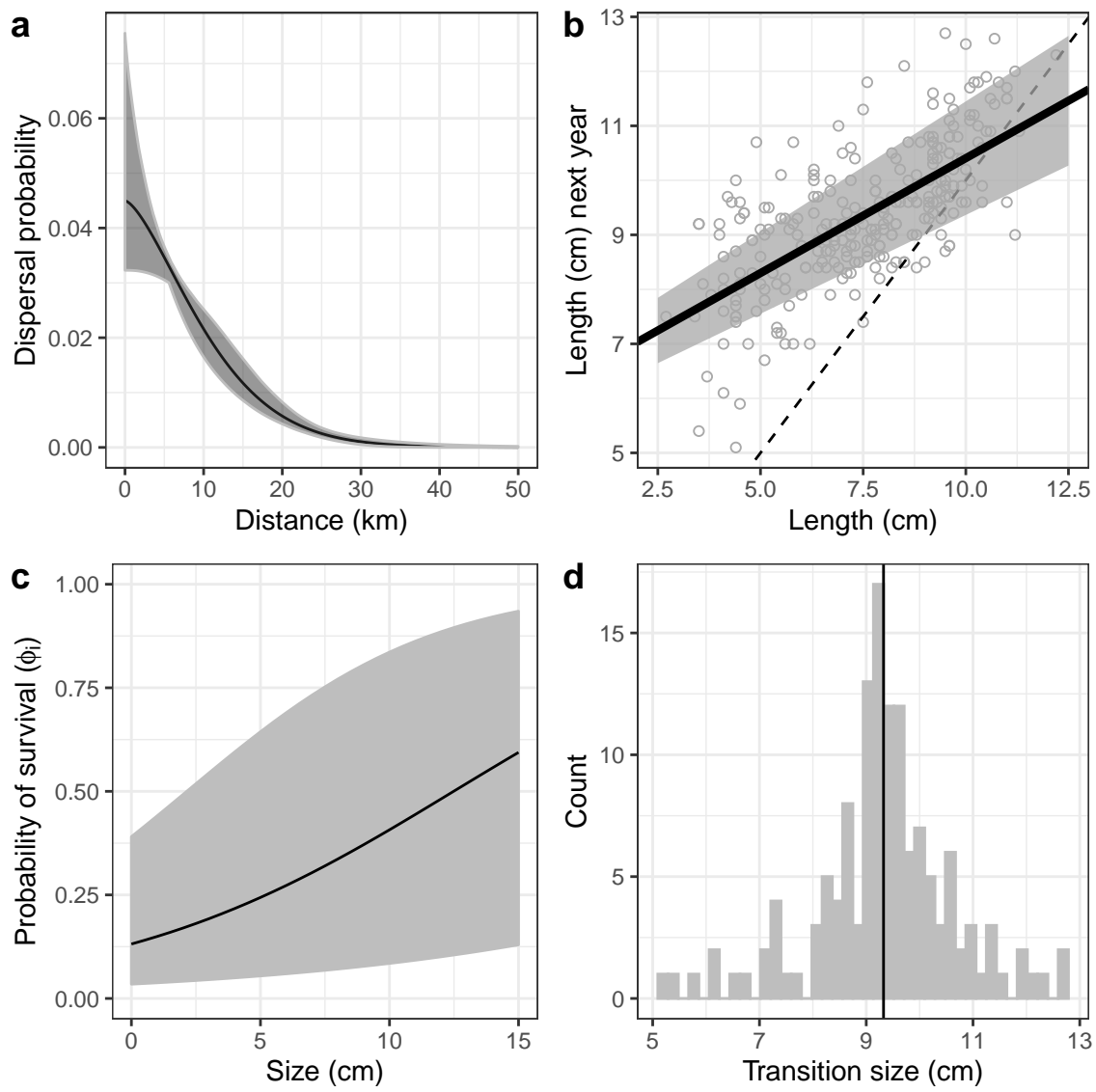


Figure 3: Estimates (solid black line) and uncertainty (grey) for a) dispersal (eqn. 5), b) growth (eqn. 6), including a dashed 1:1 line, c) post-recruit annual survival (Appendix eqn. B.1) at the example patch Elementary School, and d) raw data of fish size at female transition (L_f in Appendix eqn. A.1).

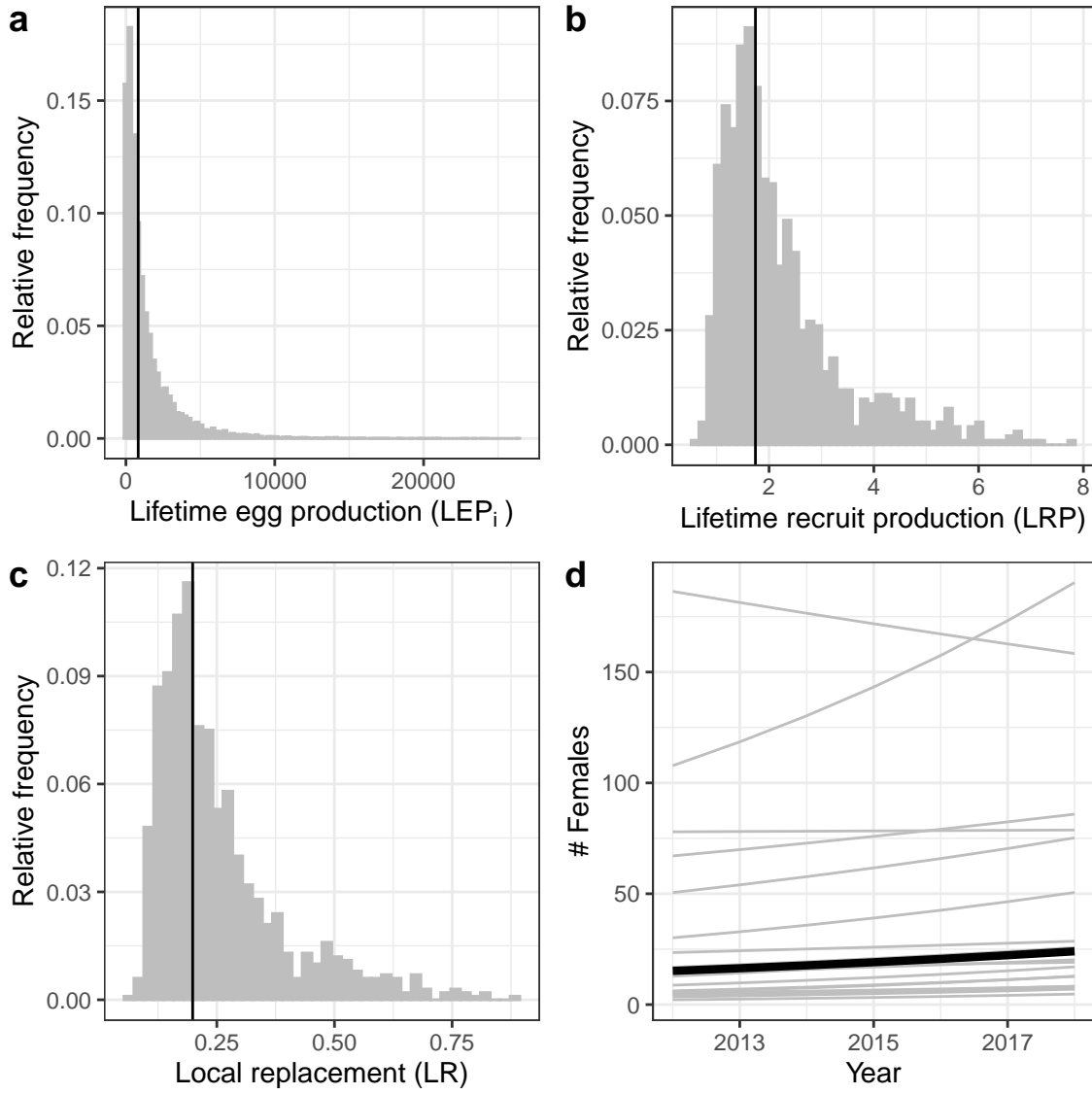


Figure 4: Estimates of a) individual-patch LEP_i (eqn. 7) for all patches with the point estimate averaged across patches (LEP_* , black line), b) average LRP across patches (eqn. 1), c) local replacement (LR, eqn. 4), showing the point estimate (black solid line) and range of estimates considering uncertainty in the inputs (grey). Estimates of LRP and LR include compensation for density-dependent mortality in early life stages. d) Estimated abundance of females over time at each individual patch (grey lines) and for an average patch (black line).

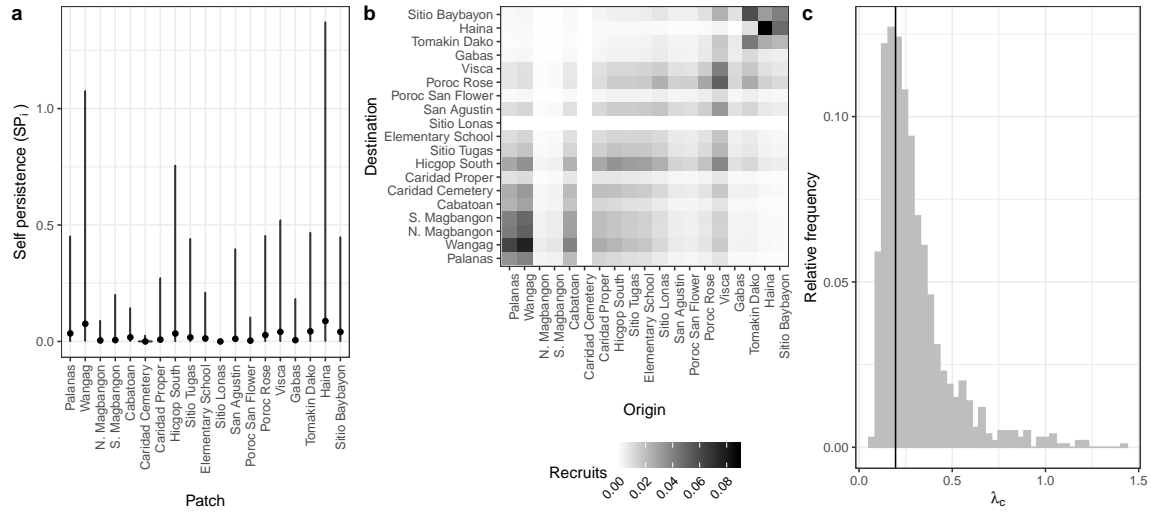


Figure 5: Values of a) self-persistence (SP_i , eqn. 2), b) realized connectivity among patches ($C_{i,j}$, eqn. 3), and c) network persistence (λ_c , first eigenvalue of eqn. 3). All estimates include compensation for density dependence in early life stages. For self-persistence (a) and network persistence (c), the best estimate is shown in black (point for (a), line for (c)) and the range of estimates considering uncertainty is shown in grey.

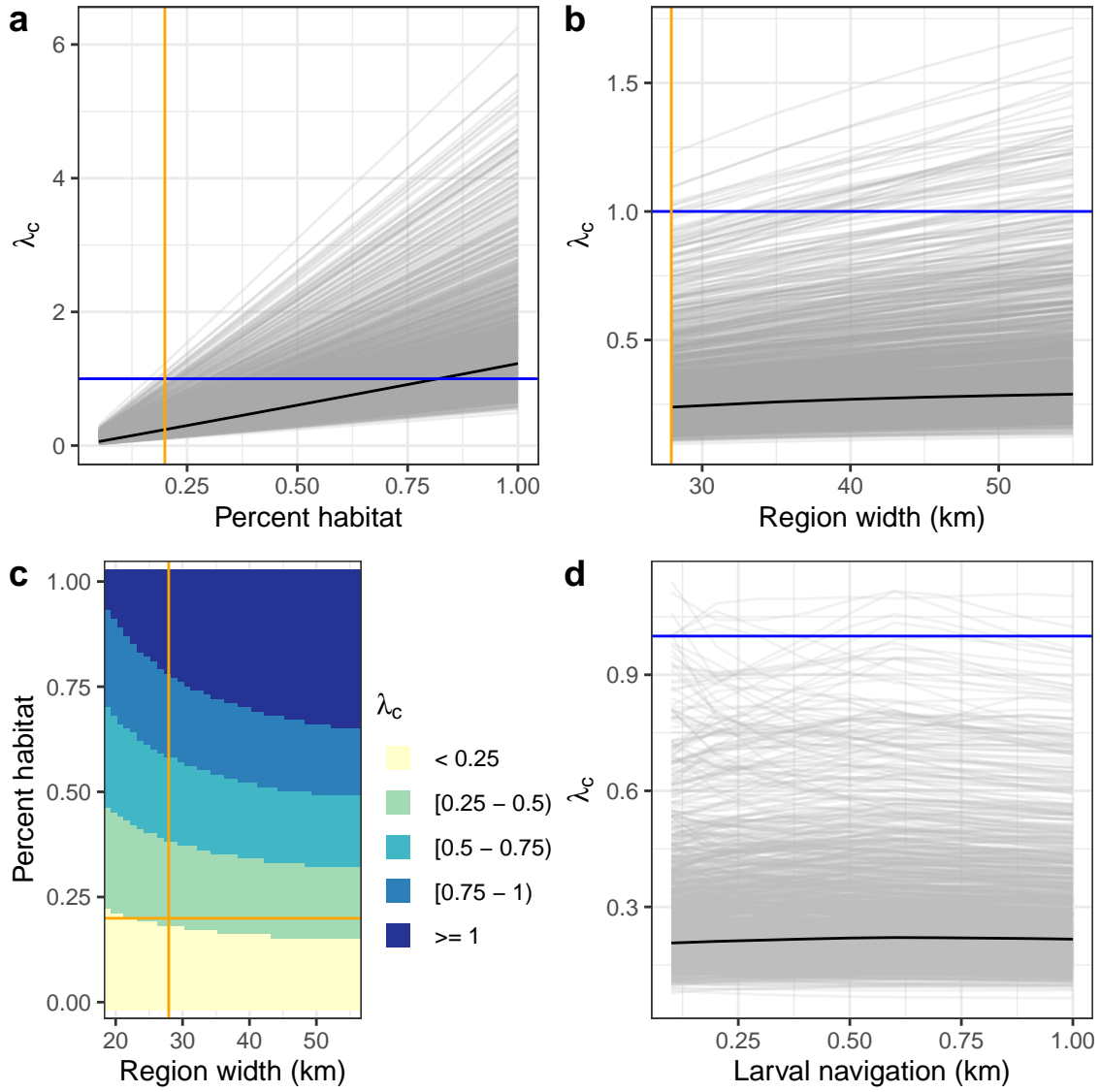


Figure 6: Sensitivity of network persistence (λ_c) to a) the proportion of the sampling region that is habitat (P_s), b) the width of a region with the same proportion habitat (20%), c) the region width and proportion habitat simultaneously, and d) larval navigation, where up to a 1 km buffer is added to the patch edges. The estimate is in black and each estimate with uncertainty is a grey line. The orange lines show the actual proportion habitat (20%) and region width (27 km) and the blue lines show the persistence threshold where $\lambda_c = 1$. Colors generated using Brewer (2020).

Appendix

A Supplemental Methods

A.1 Defining recruit and census stage

When assessing persistence, we must consider mortality and reproduction that occurs across the entire life cycle to determine whether an individual is replacing itself with an individual that reaches the same life stage (Burgess et al., 2014). We defined a recruit to be a juvenile individual that has settled on the reef within the previous year, which also encompasses the size of fish we were first able to sample (3.5–6.0 cm for parentage studies) (Fig. 1e, Appendix Fig. D.1). In theory, it does not matter how we defined recruit as long as we used the same definition in our calculations of both egg-recruit survival (eqn. 8) and LEP (eqn. 7). In our system, however, while it is straightforward to calculate LEP from any size, we did not have enough tagged recruits to reliably estimate survival from an egg to different recruit sizes. Instead, we chose the mean size of offspring matched in the parentage study as our best estimate of the size of a recruit ($\text{size}_{\text{recruit}} = 4.4 \text{ cm}$) and tested sensitivity to different recruit sizes by sampling from a uniform distribution over the sizes the recruit stage covers (3.5–6.0 cm, Appendix Table C.1, Appendix Figs. D.11-D.14).

A.2 Self persistence (SP)

Our equation for SP (eqn. 2) is a modification of that used in Burgess et al. (2014), which uses LEP to represent offspring produced and local retention (the number

of surviving recruits that disperse back to the natal patch divided by the number of eggs produced by the natal patch) to capture egg-recruit survival and dispersal combined: LEP x local retention ≥ 1 . We modify this to include egg-recruit survival in the offspring term instead, using LRP in place of LEP and probability of dispersal ($p_{i,i}$) in place of local retention.

A.3 Growth and survival

To include size in the mark-recapture models for post-recruit survival (ϕ) and recapture probability (p_r), we estimated sizes for fish in years when they were not recaptured. We used the growth model (eqn. 6) and the size recorded or estimated in the previous year to estimate the size of fish not recaptured in a particular year. Fish were not well-mixed at our patches, and divers needed to swim near an anemone to have a reasonable chance of capturing the fish on it. Therefore, we also included a distance effect on recapture probability (Appendix eqn. B.2, Appendix Table C.3). We used diver GPS tracks to estimate the minimum distance between a diver and the anemone where the fish was first caught for each tagged fish in each sample year.

We compared the fit of the models using a modified version of the Akaike information criterion that reduces the potential for overfitting with small sample sizes (AICc) and selected the model with the lowest AICc value (Appendix Table C.3).

A.4 Fecundity

We used a size-dependent fecundity relationship determined using photos of egg clutches and females from field sampling, where the number of eggs per clutch (E_c) is

exponentially related to the length in cm of the female (L) with size effect $\beta_l = 2.388$, intercept $b = 1.174$, and egg age effect $\beta_e = -0.608$ dependent on if the eggs were old enough to have visible eyes. For fish larger or equal to the transition to female size L_f , we multiplied the number of eyed eggs per clutch by the number of clutches per year $c_e = 11.9$ (estimate from Holtswarth et al., 2017) to get total annual fecundity f for a female of length L :

$$f_L = \begin{cases} 0, & \text{if } L < L_f \\ c_e * e^{\beta_l \ln(L) + \beta_e [\text{eyed}] + b}, & L \geq L_f. \end{cases} \quad (\text{A.1})$$

We did not consider uncertainty in fecundity but did consider uncertainty in the transition size to breeding female (Appendix Methods A.9).

A.5 Lifetime egg production (LEP)

To compute LEP, we discretized time and size (in eqn. 7), using 100 time steps and 100 equal size bins, and summed across the matrix. When entering the starting individual into the matrix, we used 0.1 as the standard deviation of size to spread out the starting individual across size bins. The size distribution at each time ($v_{L,t}$) represents the probability that the individual has survived and grown into each of the possible size categories. To account for differences in growth rates across fish, we used the size determined by the growth curve (eqn. 6) as the mean along with an estimate of spread (size_{sd}) when projecting the size distribution of the fish in the next year. To estimate size_{sd} , we selected fish within 0.1 cm of the mean size at the first capture point for fish recaptured a year later (7.4–7.6 cm). We used the

standard deviation of the sizes of those fish when they were recaptured one year later as size_{sd} ($=1.45$) (Appendix Table C.1).

LEP was estimated by patch (LEP_i) because each patch has a different estimate of adult survival. We also present the average LEP across patches, noted as LEP_* (Fig. 4b) and used to estimate average LRP and LR for the metapopulation (Fig. 4c, d).

To estimate egg-recruit survival (S_e), we used the expected lifetime egg production for a fish that has already survived to reach parent size (6.0 cm) so L_s in eqn. 7 = 6.0, rather than 3.5. We used the average LEP for parent-sized fish across patches, noted as LEP_p .

A.6 Accounting for density dependence

In 2015 and 2017, we did a more thorough survey of anemones at sampled patches and noted anemones occupied by yellowtail anemonefish, occupied by other species of anemonefish, and unoccupied by anemonefish. We found the proportion of anemones occupied by yellowtail anemonefish (p_A) and the proportion of anemones unoccupied by any anemonefish (p_U) for all patches combined and averaged across the two sample years. We used these average proportions to estimate the proportional increase (D) in unoccupied anemones if all anemones occupied by yellowtail anemonefish were unoccupied as described in the main text. We did not consider uncertainty in the effect of density dependence.

A.7 Alternative geographies and larval navigation

Larval navigation

In our sensitivity test for larval navigation and swimming abilities, we added a buffer ranging from 0–1 km to the edges of the destination patches when determining probability of dispersal between patches. To avoid overlapping shadows of effective area of neighboring patches, we added no more than half the distance between two adjacent patches to each patch. The buffers also changed the proportion of the sampling region that was habitat (P_h , see Appendix Methods A.8), as we considered the buffer areas to be habitat as well, and affected the scaling of recruits (Appendix Methods A.8) in egg-recruit survival (eqn. 8).

A.8 Scaling up recruits

To estimate the total number of offspring produced by genotyped parents that survived to recruitment, we scaled up the number of matched offspring caught during sampling (R_m) to account for recruits our sampling could have missed (Appendix Fig. D.2). We scaled up by 1) the cumulative proportion of habitat we sampled at our patches over time (P_h) to account for recruits at anemones we did not sample, 2) the probability of capturing a fish if we sampled its anemone (P_c) to account for fish that escaped during sampling, 3) the proportion of the dispersal kernel from our patches covered within our sampling region (P_d) to account for fish that dispersed outside of our sampling area (Appendix Fig. D.4), and 4) the proportion of our sampling region that was habitat (P_s) to avoid counting mortality of fish dispersing to

non-habitat within our region twice. The latter term is important because mortality from dispersing to non-habitat is both in the estimate of total recruits (numerator of eqn. 8) and in the integrated dispersal kernel (eqn. 5).

Proportion of habitat sampled (P_h)

We used tagged anemones to estimate the proportion of habitat we sampled within our patches (Appendix Table C.4). We tagged each anemone that was home to yellowtail anemonefish with a metal tag, which is relatively permanent and easy to re-sight (the anemone tag is visible above the anemone in Fig. 2c). We therefore considered the total number of metal-tagged anemones at a patch to be the habitat present. We used proportion of anemones rather than proportion of total patch area because anemones, and therefore habitat quality, were unevenly distributed across each patch; areas we did not visit typically had a lower anemone density than the areas we did sample.

To scale the number of sampled offspring from genotyped parents (R_m) to account for areas of our patches we did not sample, we used the overall proportion habitat sampled across all patches and sampling years (P_h). We summed the number of metal-tagged anemones we visited across all patches and years, then divided by the number of anemones we could have sampled (the sum of total metal-tagged anemones across all patches multiplied by the number of sampling years) (anemone numbers sampled by patch and year in Appendix Table C.4). We did not consider uncertainty in the proportion of habitat sampled.

Probability of capturing a fish, from recapture dives (P_c)

We used the probability of capturing a fish to scale up the number of sampled offspring from genotyped parents (R_m) to account for recruits we missed by failing to capture them. To estimate the probability of capturing a fish given that we sampled its anemone (P_c), we used mark-recapture data from recapture dives done within a sampling season. During some of the sampling years, we intentionally re-sampled some locations within a few weeks of the original sampling dives. We assumed that the probability of recapturing a fish on a recapture dive was the same as capturing a fish on a sampling dive, essentially that there was no mortality in the weeks between dives and that the fish did not alter their behavior towards divers. For each recapture dive, we used GPS tracks of the divers to identify the anemones covered in the recapture dive and the set of PIT-tagged fish encountered on those anemones during the original sampling dives. We estimated the probability of capture P_c as the number of tagged fish re-caught from the capture dive m_2 divided by the total number of fish caught on the recapture dive n_2 : $P_c = \frac{m_2}{n_2}$.

We used the mean P_c across all 14 recapture dives, covering 10 patches over three sampling seasons (2016, 2017, 2018), as our best estimate. Uncertainty details are in Appendix Methods A.9.

Proportion of dispersal kernel area sampled (P_d)

To account for recruits that dispersed outside our sampling region, we found the proportion of the dispersal kernels from all parents that fell within our sampling

region (Appendix Fig. D.4). For each patch i , we found the area under the kernel (A_i) from the center of the patch to the north edge of the sampling area ($d_{N,i}$) (northern-most tagged anemone at Palanas, the northern-most patch) and from the center of the patch to the south edge of the sampling area ($d_{S,i}$) (southern-most tagged anemone at Sitio Baybayon, the southern-most patch), then multiplied by the number of genotyped parents at that patch (N_{g_i}):

$$A_i = N_{g_i} \frac{e^{K_d \theta}}{2\Gamma(\frac{1}{\theta})} \left(\int_0^{d_N} e^{-(e^{K_d d})^\theta} dd + \int_0^{d_S} e^{-(e^{K_d d})^\theta} dd \right). \quad (\text{A.2})$$

We added the areas together, then divided by the total number of genotyped parents (N_g) to get the proportion of the total dispersal kernel area covered by our sampling region (P_d):

$$P_d = \frac{\sum_{i=1}^{19} A_i}{N_g}. \quad (\text{A.3})$$

We did not consider uncertainty in P_d .

Proportion habitat in sampling area (P_s)

To avoid implicitly counting mortality due to larvae settling on non-habitat twice — once in scaling up our matched recruits (who settled on habitat) and once in integrating the dispersal kernel — we scaled the estimate of total recruits produced by parents on our patches by the proportion of our sampling region that was habitat (P_s). We found P_s by summing the lengths of all the patches, which run approximately north-south, and dividing by the total north-south distance of our sampling

region, giving $P_s = 0.20$. We assumed that larvae were unable to navigate to habitat if they dispersed to an unsuitable area but relaxed that assumption in our sensitivity tests (Appendix Methods A.7) because anemonefish larvae do likely have some ability both to sense good settlement areas by detecting host anemones (Elliott et al., 1995; Arvedlund et al., 1999) or conspecifics (e.g., Lecchini et al., 2005, for coral reef fish more broadly), and to swim in a particular direction (e.g., Bellwood and Fisher, 2001; Fisher, 2005).

A.9 Characterizing uncertainty

Dispersal kernel

To account for uncertainty in the dispersal kernel, we used sets of the shape parameter θ and the scale parameter K_d that represented the span of the 95% confidence interval when K_d and θ were estimated jointly (Appendix Table C.1, Fig. 3a, Catalano et al., in review). We randomly sampled pairs of θ and K_d parameters from within the 95% confidence intervals, weighted by the log-likelihood.

Growth

We used the first and second capture lengths for fish that were recaptured after a year (within 345 to 385 days) to estimate L_∞ and k (using eqn. 6). For fish recaptured more than once, we randomly selected only one recapture period from each to use to estimate the von Bertalanffy parameters and repeated the random selection and estimate 1000 times. We found the mean estimates ($L_\infty = 10.70$ cm, $k = 0.864$) and mean standard error of those fits, then sampled uniformly from within the average

95% range to generate a set of von Bertalanffy growth curves to use in our LEP calculations (Fig. 3b, Appendix Fig. D.3b, Appendix Table C.1).

Survival (ϕ)

We incorporated uncertainty in adult survival by sampling uniformly from within the 95% confidence limits for the patch-based survival estimates and size effect on survival as estimated by the lowest AICc model from MARK (Appendix Table C.2, Appendix Fig. D.5). For the simulations for the alternative geographies and larval navigation, we used the survival estimate and 95% range for the patch with median survival (the Elementary School patch) (Appendix Table C.1).

Size of transition to female (L_f)

To incorporate uncertainty in the size at which male fish transition to female (L_f), we sampled with replacement directly from the sizes at which recaptured fish were first captured as female (5.2–12.7 cm) (Fig. 3d). Reproductive output is only counted once fish reach the female stage, so L_f affects fecundity (Appendix eqn. A.1) and therefore the fecundity kernel in calculating lifetime egg production (f_L in eqn. 7).

Recruit size (size_{recruit})

We incorporated uncertainty in the size of a recruit (size_{recruit}) by sampling from a uniform distribution across the ranges of possible sizes of recruits for the parentage analysis (3.5–6.0 cm) (Appendix Fig. D.3a). Recruit size enters into LEP as the starting size of the individual fish in eqn. 7.

Probability of capturing a fish (P_c)

To consider uncertainty in the probability of capturing a fish given that we sampled its anemone (P_c), we represented the probability of capture as a beta distribution, using the mean μ_{P_c} and variance V_{P_c} of the set of 14 values calculated from individual recapture dives to find the appropriate α_{P_c} and β_{P_c} parameters, where

$$\alpha_{P_c} = \left(\frac{1 - \mu_{P_c}}{V_{P_c}} - \frac{1}{\mu_{P_c}} \right) \mu_{P_c}^2 \quad (\text{A.4})$$

$$\beta_{P_c} = \alpha_{\mu_{P_c}} \times \frac{1}{\mu_{P_c} - 1}. \quad (\text{A.5})$$

The mean of the individual capture probability values was $\mu_{P_c} = 0.56$, with variance $V_{P_c} = 0.069$, giving beta distribution parameters $\alpha_{P_c} = 1.44$ and $\beta_{P_c} = 1.13$. We sampled 1000 values from the beta distribution, then truncated the sample to include only values larger or equal to the lowest value of P_c estimated from an individual dive (0.20), to avoid unrealistically low values randomly sampled from the distribution. We then sampled with replacement from the truncated set to get a vector of 1000 values (Appendix Fig. D.3c). P_c is one of the scaling factors in the estimate of egg-recruit survival (eqn. 8), accounting for recruits we missed by failing to capture them.

Lifetime Egg Production (LEP)

Uncertainty in lifetime egg production enters through adult survival, growth, and the size of a recruit (Appendix Methods A.9), all of which affect the size distribution across time $v_{L,t}$ in eqn. 7. Additionally, uncertainty in the size of transition to female (L_f , Appendix Methods A.9) affects the fecundity kernel f_L in eqn. 7. We show the contribution of uncertainty of each input in Appendix Fig. D.11.

Egg-recruit survival (S_e)

In estimating egg-recruit survival (S_e), we considered uncertainty in the number of offspring assigned to parents (R_m) and in the probability of capturing a fish (P_c). For offspring assigned to parents, we generated a set of values for the number of assigned offspring using a random binomial, with the number of genotyped offspring (791) as the number of trials and the assignment rate from the parentage analysis (0.090) as the probability of success on each trial (Catalano et al., in review) (Appendix Fig. D.3d). Uncertainty in probability of capture P_c is described in Appendix Methods A.9. We show the contribution of uncertainty of each input in Appendix Fig. D.13.

B Supplemental Results

B.1 Parentage

From the genetic work and parentage analysis done in Catalano et al. (in review), we genotyped 1729 potential parents, genotyped 791 potential offspring (recruits), and matched 71 offspring to parents, with an assignment rate of 9%. In estimates with uncertainty, the middle 95% of the distribution of matched offspring was 55 to 87 (Appendix Fig. D.3d, Appendix Table C.1).

The combined number of potential parents and potential offspring is higher than the number of genotyped fish because some fish are included as both a potential offspring and a potential parent (in different years).

B.2 Dispersal kernel

We used the dispersal kernel estimated for all years together in Catalano et al. (in review) (eqn. 5), with $K_d = -2.51$ and $\theta = 1.49$. Using the 95% confidence surface when K_d and θ were estimated jointly to incorporate uncertainty (Appendix Methods A.9), K_d ranged from -2.86 to -1.82 and θ from 0.87 to 2.46 (Fig. 3a, Appendix Table C.1).

B.3 Growth

From the mark-recapture analysis of tagged and genotyped fish, we estimated mean values of $L_\infty = 10.70$ cm with uncertainty bounds of 9.0–12.8 cm using the 95% confidence bounds with average standard error across fits and $k = 0.864$ with un-

certainty bounds 0.73–1.01 for the von Bertalanffy growth curve parameters (eqn. 6, Fig. 3b, Appendix Table C.1).

B.4 Survival

The best model for post-recruitment annual survival ϕ on a log-odds scale had a positive size effect ($b_a = 0.15 \pm 0.029$ SE) with intercepts b_{ϕ_i} varying by patch (Appendix eqn. B.1, Appendix Fig. D.5, Appendix Table C.2):

$$\ln\left(\frac{\phi}{1-\phi}\right) = b_{\phi_i} + b_a \text{size}. \quad (\text{B.1})$$

The accompanying best model for recapture probability p_r on a log-odds scale had a negative effect of size ($b_1 = -0.16 \pm 0.09$ SE) and a negative effect of diver distance d from the capture anemone ($b_2 = -0.15 \pm 0.02$ SE), with intercept $b_{p_r} = 2.14 \pm 0.87$ SE (Appendix eqn. B.2, Appendix Fig. D.6):

$$\ln\left(\frac{p_r}{1-p_r}\right) = b_{p_r} + b_1 \text{size} + b_2 d. \quad (\text{B.2})$$

This suggests divers were less likely to recapture larger fish, who are stronger swimmers and more likely to flee when divers approach, and those at anemones far from areas sampled.

B.5 Scaling factors

The proportion of habitat at patches sampled over time (P_h) was 0.41, the proportion of the region that was habitat (P_s) was 0.20, the proportion of the dispersal kernel

that was within the sampling region (P_d) was 0.57, and the probability of capturing a fish given that its anemone was sampled (P_c) was 0.56, with middle 95% 0.22–0.97 (Appendix Fig. D.3c, Appendix Table C.1).

B.6 Lifetime egg production (LEP)

We calculated an average value of LEP across patches (LEP_*) of 827 [266, 3213] eggs (Fig. 4a), with best estimate values at individual patches that ranged from 0 to 1760 eggs (Appendix Table C.5). Uncertainty in adult survival had the largest effect on LEP (Appendix Fig. D.11), which corresponds to longer-surviving individuals having more opportunities to reproduce at larger sizes.

B.7 Egg-recruit survival (S_e)

We estimated egg-recruit survival S_e to be 0.002 [5×10^{-4} , 0.01] when we accounted for density dependence in our data. Uncertainty in the size of transition to breeding female L_f had the largest effect on egg-recruit survival (Appendix Fig. D.13); the larger the transition size to female, the fewer tagged eggs we estimated were produced by our genotyped parents and the higher the estimate of egg-recruit survival. This differs from our finding above that adult survival had the largest effect on LEP because the starting size of the individual considered is lower when we estimate LEP for a recruit (4.4 cm, 3.5–6.0 cm range) than for a parent (6.0 cm). Fish considered parents in our parentage analysis have already survived one or more years since recruiting so the transition to breeding female plays a larger role in the number of eggs they are likely to produce than for fish who have just recruited.

B.8 Persistence metrics without compensation for density dependence

Estimating persistence metrics without compensating for density dependence in our data (presented with a subscript D) gave us an understanding of whether individuals at our patches were able to replace themselves and whether our patches would persist in isolation at the current abundance levels, rather than at low abundance. Without compensation for early life density dependence, all of our metrics showed that the set of patches we sampled was less likely to persist as an isolated network than the metrics for low abundance. We estimated egg-recruit survival (S_{eD}) to be 0.001 [3×10^{-4} , 0.005] and average lifetime recruit production across patches (LRP_D) to be 0.96 [0.51, 3.07], with 52% of LRP_D estimates ≥ 1 (Appendix Fig. D.9a). Our estimate of local replacement (LR_D), which estimates replacement for recruits from our patches returning to our patches implicitly including dispersal, was 0.11 [0.06, 0.35] (Appendix Fig. D.9b).

When we calculated LR using all arriving recruits to our patches, however, rather than just those originating there, the best estimate was > 1 (1.22), suggesting that there was recruit-recruit replacement at our patches when we included immigrant recruits, even at current population levels when density dependence was present.

We did not find any patches with a best estimate of SP_D ≥ 1 or with uncertainty bounds that reached or exceeded 1 (Appendix Figs. D.10a). Our best estimate of the dominant eigenvalue of the realized connectivity matrix λ_{cD} was 0.11 [0.06, 0.47] with 0% of estimates where $\lambda_{cD} \geq 1$ (Appendix Fig. D.10c).

C Supplemental Tables

Table C.1: Summary of parameter symbols, definitions, and values, including sections and equations where each is described in detail.

Parameter	Description	Best estimate (uncertainty bounds)	Uncertainty origin	Details	Notes
<i>Dispersal and demographics</i>					
K_d	scale parameter in dispersal kernel	-2.51 (-2.86, -1.82)	drawn from joint 95% confidence limits with θ , weighted by log-likelihood	eqn. 5, Appendix Methods A.9, Appendix Results B.2	estimated in Cata-lano et al. (in review)
θ	shape parameter in dispersal kernel	1.49 (0.87, 2.46)	drawn from joint 95% confidence limits with K_d , weighted by log-likelihood	eqn. 5, Appendix Methods A.9, Appendix Results B.2	estimated in Cata-lano et al. (in review)
L_∞	average asymptotic size (cm) in von Bertalanffy growth curve	10.7 cm (9.0, 12.8)	average 95% confidence limits of growth curves estimated with different pairs of fish	eqn. 6, Appendix Methods A.3, A.9, Appendix Results B.3	
k	growth coefficient in von Bertalanffy growth curve	0.864 (0.732, 1.01)	average 95% confidence limits of growth curves estimated with different pairs of fish	eqn. 6, Appendix Methods A.3, A.9, Appendix Results B.3	

	size _{recruit}	size of a recruit	4.4 cm (3.5–6.0)	sampled from a uniform distribution to match the range of offspring sizes for parent-age analyses	Appendix Methods A.1, A.9	used as starting size of fish in calculation of LEP (eqn. 7)
	b	intercept at 0 cm for size-fecundity relationship	1.174 eggs	no uncertainty	Appendix eqn. A.1, Appendix Methods A.4	
	β_l	size effect for size-fecundity relationship	2.388 $\frac{\text{eggs}}{\text{cm}}$	no uncertainty	Appendix eqn. A.1, Appendix Methods A.4	
	β_e	egg age effect in fecundity	-0.608	no uncertainty	Appendix eqn. A.1, Appendix Methods A.4	egg age was determined by the presence of visible eyes (eyed vs. non-eyed)
	c_e	number of egg clutches per year	11.9	no uncertainty	Appendix eqn. A.1, Appendix Methods A.4	Holtswarth et al. (2017)
	size _{sd}	spread in sizes of fish one year later	1.45	no uncertainty	used in estimating LEP, Appendix Methods A.5	estimated from recapture data

parent size	size of fish used to estimate LEP for parents (LEP _p)	6.0 cm	no uncertainty	Appendix Methods A.5	used in estimating egg-recruit survival (S_e , eqn. 8)
R_m	number of offspring matched to genotyped parents	71 [55, 87]	middle 95% of distribution from random binomial for each genotyped offspring using the assignment rate from the parentage analysis (9%)	Appendix Methods A.9	used in calculating egg-recruit survival (S_e , eqn. 8)
genotyped offspring	number of recruits genotyped	791	no uncertainty	Appendix Results B.1	used to find mean recruit size (size _{recruit}), estimate metrics with immigrants included
N_g	potential parents genotyped	1729	no uncertainty	Appendix Results B.1	used to find proportion of dispersal kernel area sampled (P_d , Appendix Methods A.8), egg-recruit survival (S_e , eqn. 8)
L_f	size of transition to female	9.3 cm (5.2, 12.7)	sampled with replacement from transition sizes for recaptured fish	Appendix eqn. A.1, Appendix Methods A.9	used to find fecundity (Appendix eqn. A.1)

$b_{\phi,i=ES}$	intercept at size = 0 cm for survival at Elementary School patch	-1.88 (-3.33, -0.44)	sampled from within 95% confidence limits from MARK estimates	Appendix eqn. B.1, Appendix Methods A.3, A.9, Appendix Results B.4	patch with median survival, used in proportion habitat, region width, and larval navigation sensitivity tests
b_a	size effect for survival	0.15 (0.10, 0.21)	sampled from within 95% confidence limits from MARK estimates	Appendix eqn. B.1, Appendix Methods A.3, A.9, Appendix Results B.4	
<i>Scaling factors</i>					
D	proportional increase in unoccupied anemones to account for density-dependence at settlement	1.18	no uncertainty	section “Accounting for density-dependence”, Appendix Methods A.6	used to scale recruits for egg-recruit survival (S_e , eqn. 8)
p_A	proportion anemones occupied by yellow-tail anemonefish	0.37	no uncertainty	Appendix Methods A.6	
p_U	proportion anemones unoccupied by anemonefish	0.46	no uncertainty	Appendix Methods A.6	

P_h	cumulative proportion of habitat in patches sampled	0.41	no uncertainty	Appendix Methods A.8	used to scale recruits for egg-recruit survival (S_e , eqn. 8)
P_s	proportion of region that was habitat	0.20	no uncertainty	Appendix Methods A.8	used to scale recruits for egg-recruit survival (S_e , eqn. 8)
P_d	proportion dispersal kernel area in sampling region	0.57	no uncertainty	Appendix Methods A.8	used to scale recruits for egg-recruit survival (S_e , eqn. 8)
P_c	probability of capturing a fish	0.56	sampled from a beta distribution	Appendix Methods A.8, A.9	used to scale recruits for egg-recruit survival (S_e , eqn. 8)

Table C.2: Table with patch-specific survival values (ϕ_i) on a log-odds scale (used in Appendix eqn. B.1), where the intercept is for post-recruit survival for a fish of size 0 cm. The intercept for each patch is the intercept for Cabatoan plus the additional intercept value for that patch, shown in the table.

Patch	Intercept	Standard error	Confidence limits	Notes
Cabatoan	-1.78	0.33	-2.42 to -1.14	
Caridad Cemetery	-19.66	0.00	-19.66 to -19.66	addition to Cabatoan intercept
Elementary School	-0.11	0.41	-0.92 to 0.69	addition to Cabatoan intercept
Gabas	-0.42	0.58	-1.55 to 0.72	addition to Cabatoan intercept
Haina	0.12	0.35	-0.57 to 0.81	addition to Cabatoan intercept
Higcop South	-0.06	0.46	-0.96 to 0.84	addition to Cabatoan intercept
N. Magbangon	-1.31	0.38	-2.05 to -0.57	addition to Cabatoan intercept
Palanas	0.24	0.26	-0.26 to 0.75	addition to Cabatoan intercept
Poroc Rose	-0.19	0.44	-1.05 to 0.68	addition to Cabatoan intercept
Poroc San Flower	-0.52	0.48	-1.45 to 0.42	addition to Cabatoan intercept
San Agustin	-0.47	0.50	-1.45 to 0.42	addition to Cabatoan intercept
Sitio Baybayon	0.02	0.26	-0.49 to 0.52	addition to Cabatoan intercept
S. Magbangon	-1.08	0.48	-2.02 to -0.14	addition to Cabatoan intercept
Tomakin Dako	0.39	0.33	-0.25 to 1.03	addition to Cabatoan intercept
Visca	0.33	0.35	-0.36 to 1.01	addition to Cabatoan intercept
Wangag	0.35	0.25	-0.15 to 0.85	addition to Cabatoan intercept

Table C.3: Table showing the set of models considered in MARK for survival (ϕ , from Appendix eqn. B.1) and recapture probability (p_r , from Appendix eqn. B.2), including effects of fish size (L), minimum distance from diver to the anemone where the fish was first caught during surveys (D_m), year (t), and patch (i), and their relative AICc scores.

Model	Model description	AICc	dAICc
$\phi \sim L + i, p_r \sim L + D_m$	survival: size + patch, recapture: size + distance	3104.1	0
$\phi \sim i, p_r \sim L + D_m$	survival: patch, recapture: size + distance	3127.2	23.1
$\phi \sim i, p_r \sim D_m$	survival: patch, recapture: distance	3127.2	23.1
$\phi \sim L, p_r \sim L + D_m$	survival: size, recapture: size + distance	3139.9	35.8
$\phi \sim L, p_r \sim D_m$	survival: size, recapture: distance	3141.6	37.5
$\phi, p_r \sim L + D_m$	survival: constant, recapture: size + distance	3168.4	64.3
$\phi, p_r \sim D_m$	survival: constant, recapture: distance	3169.3	65.2
$\phi \sim t, p_r$	survival: time, recapture: constant	3243.9	139.8
$\phi \sim i, p_r$	survival: patch, recapture: constant	3254.4	150.3
$\phi, p_r \sim t$	survival: constant, recapture: time	3274.0	169.9
$\phi \sim L, p_r \sim L$	survival: size, recapture: size	3345.1	241.0
ϕ, p_r	survival: constant, recapture: constant	3382.7	278.6

Table C.4: Table showing the percent of anemones surveyed at each patch, ordered from north to south, in each sampling year.

		% Habitat surveyed						
Patch	# Total anems	2012	2013	2014	2015	2016	2017	2018
Palanas	138	29	57	48	61	85	86	86
Wangag	291	18	33	42	35	27	49	69
N. Magbangon	105	5	12	40	63	64	0	5
S. Magbangon	34	41	56	32	0	65	0	71
Cabatoan	26	42	58	58	65	73	0	62
Caridad Cemetery	4	0	75	50	0	50	50	50
Caridad Proper	4	0	100	0	0	0	0	0
Hicgop South	18	0	67	28	28	56	83	78
Sitio Tugas	8	0	100	0	0	0	0	0
Elementary School	7	0	100	43	100	100	86	100
Sitio Lonas	1	100	100	0	0	0	0	0
San Agustin	18	89	61	72	61	100	89	72
Poroc San Flower	11	100	82	73	73	55	82	64
Poroc Rose	13	100	100	69	31	23	69	69
Visca	13	100	100	23	38	62	85	62
Gabas	9	0	0	0	44	44	67	0
Tomakin Dako	48	0	25	23	38	35	60	69
Haina	104	0	6	13	13	10	56	80
Sitio Baybayon	259	0	14	30	34	30	41	81
Overall	1111	16	32	36	39	42	48	67

Table C.5: Table showing patch-specific estimates of lifetime egg production (LEP_i), lifetime recruit production (LRP_i), and self persistence (SP_i)

Patch	LEP_i	LRP_i	SP_i
Palanas	1383	2.91	0.03
Wangag	1642	3.45	0.08
N. Magbangon	133	0.28	0.004
S. Magbangon	183	0.39	0.006
Cabatoan	933	1.96	0.02
Caridad Cemetery	0	0	0
Caridad Proper	781	1.64	0.008
Hicop South	848	1.78	0.03
Sitio Tugas	781	1.64	0.02
Elementary School	781	1.64	0.01
Sitio Lonas	781	1.64	0
San Agustin	445	0.92	0.01
Poroc San Flower	415	0.87	0.004
Poroc Rose	694	1.46	0.03
Visca	1586	3.34	0.04
Gabas	483	1.02	0.006
Tomakin Dako	1760	3.70	0.04
Haina	1130	2.38	0.09
Sitio Baybayon	959	2.02	0.04

D Supplemental Figures

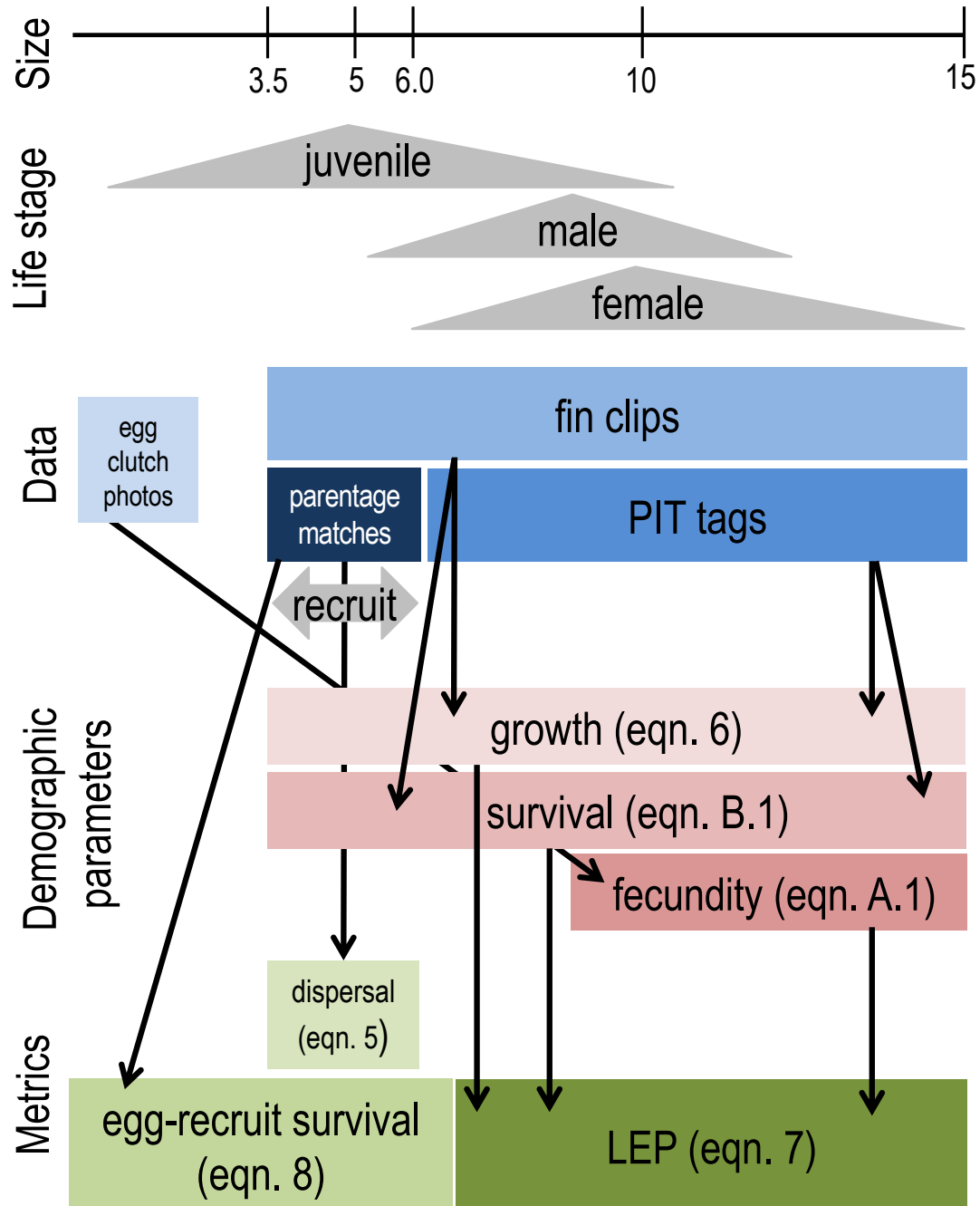


Figure D.1: The data collected for fish at each life stage and how they match to the equations and metrics estimated. We considered recruits to be offspring in their first year of settlement, represented by the 3.5–6.0 cm size range (Appendix Methods A.1).

How could we have missed potential recruits originating from our patches?

- 1) Failed to catch recruit when sampling (P_c)
- 2) Missed sampling some habitat areas within our patches (P_h)
- 3) Recruit dispersed outside our study region (P_d)
- 4) Recruit dispersed to non-habitat within our region (P_s)
- 5) Recruit died due to density-dependent competition with other settlers (D)

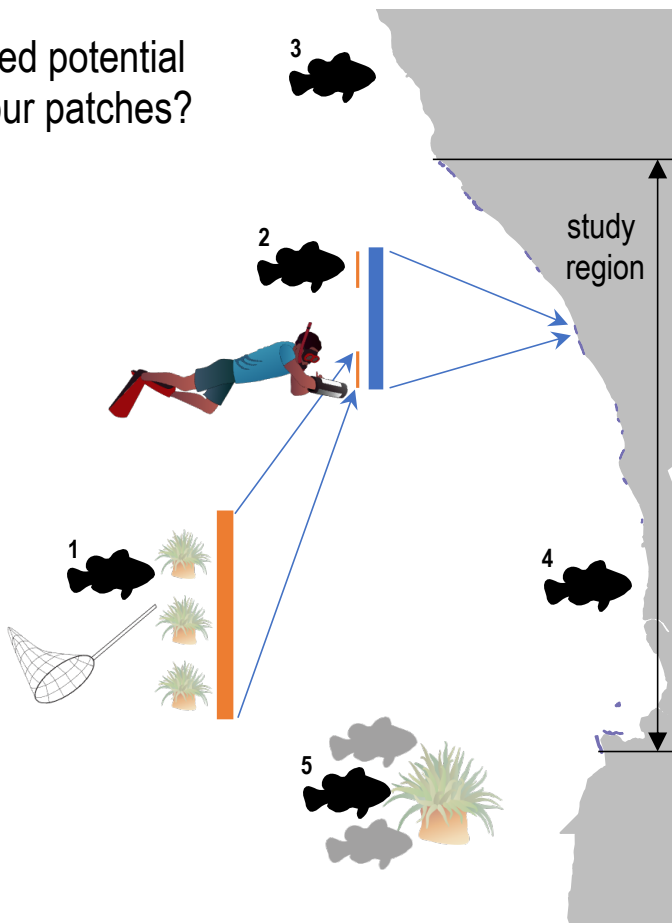


Figure D.2: Schematic of five ways we could have missed recruits while sampling. We used these factors to scale up our raw estimate of recruits from matched offspring (Appendix Methods A.8).

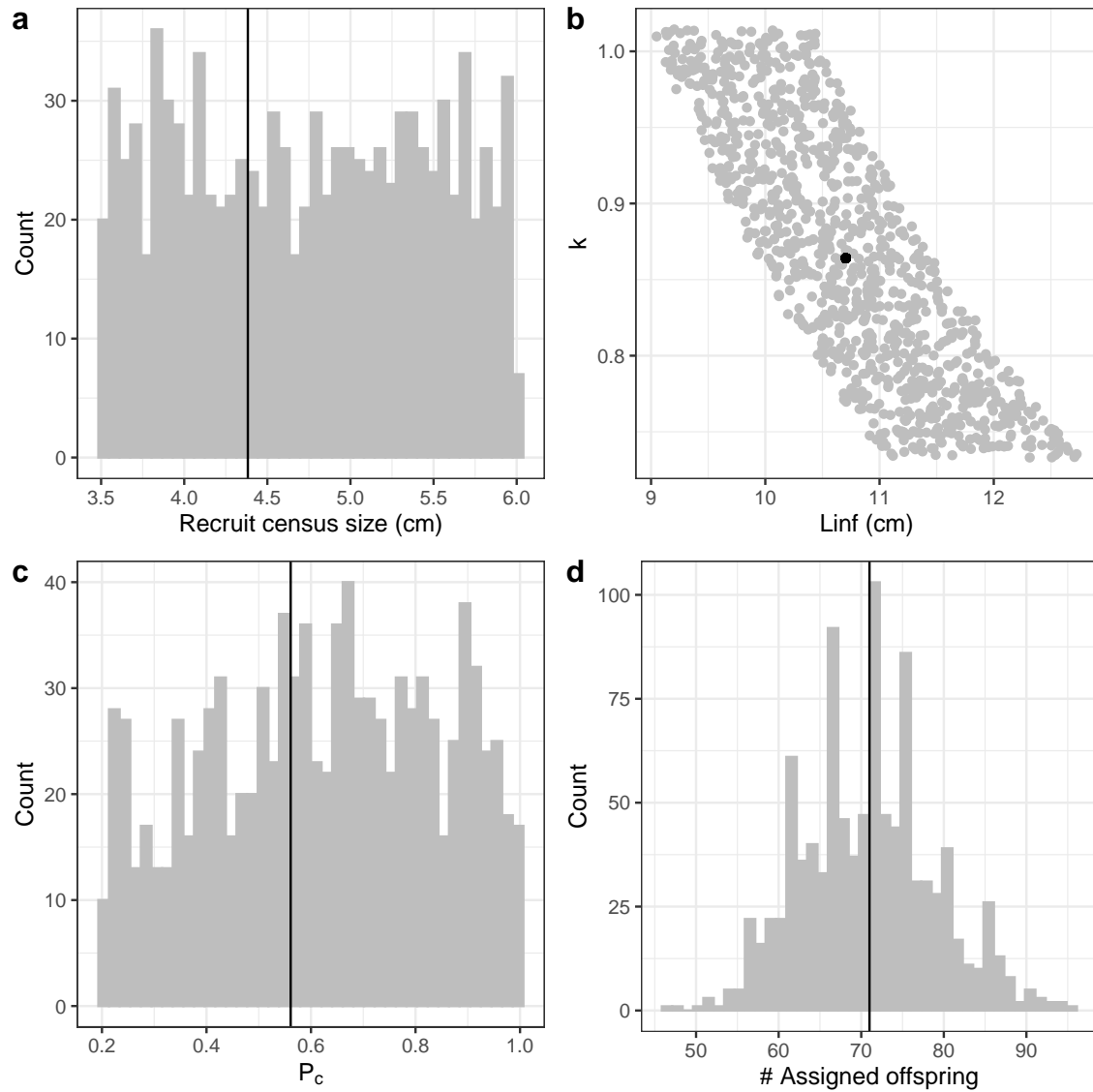


Figure D.3: Range of parameter inputs for uncertainty runs with all uncertainty included, where the black line or point is the value used for the best estimate: a) $\text{size}_{\text{recruit}}$, the census size for recruits after egg-recruit survival; b) the parameters L_{∞} and k of the von Bertalanffy growth model; c) P_c , the probability of capturing a fish; d) R_m , the number of offspring assigned back to parents in the parentage analysis.

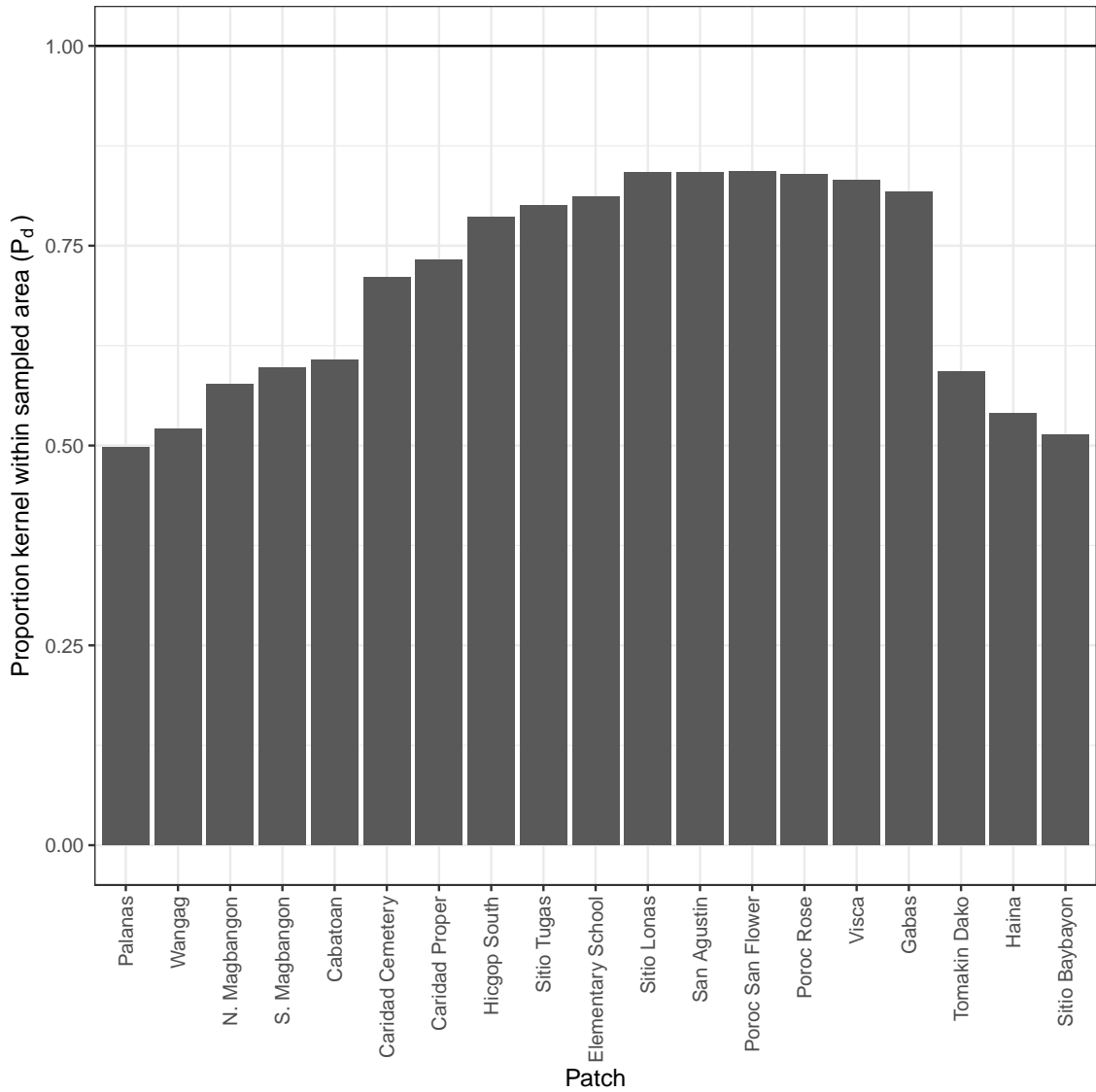


Figure D.4: Proportion of the dispersal kernel area from the center of each patch covered by our sampling region ($\frac{A_i}{N_{g,i}}$ from Appendix eqn. A.3). The overall proportion (P_d) is weighted by the number of parents at each patch.

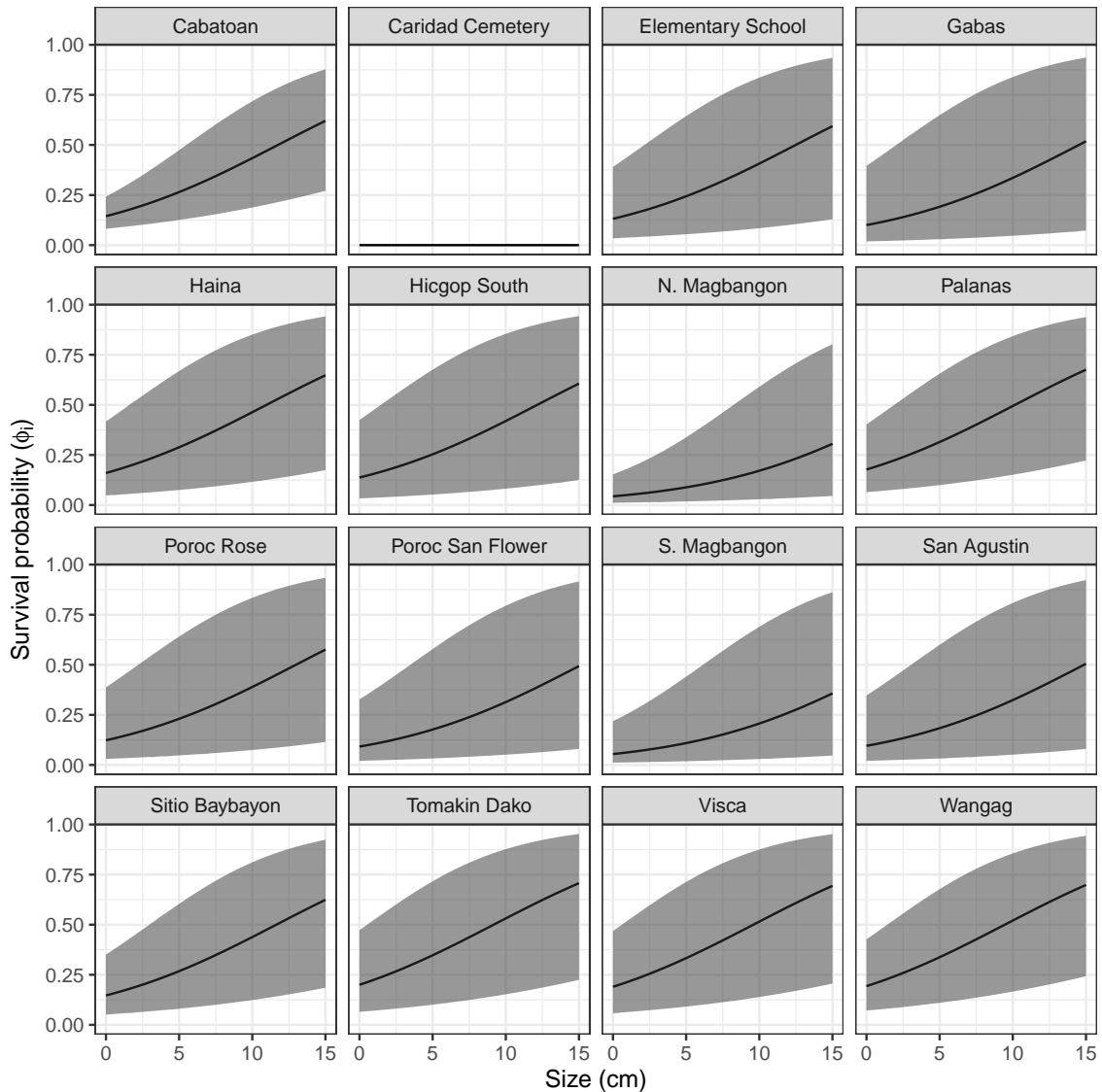


Figure D.5: Annual post-recruit survival (ϕ) by fish size at each patch, detailed in Appendix Methods A.3, A.9, and Appendix Results B.4.

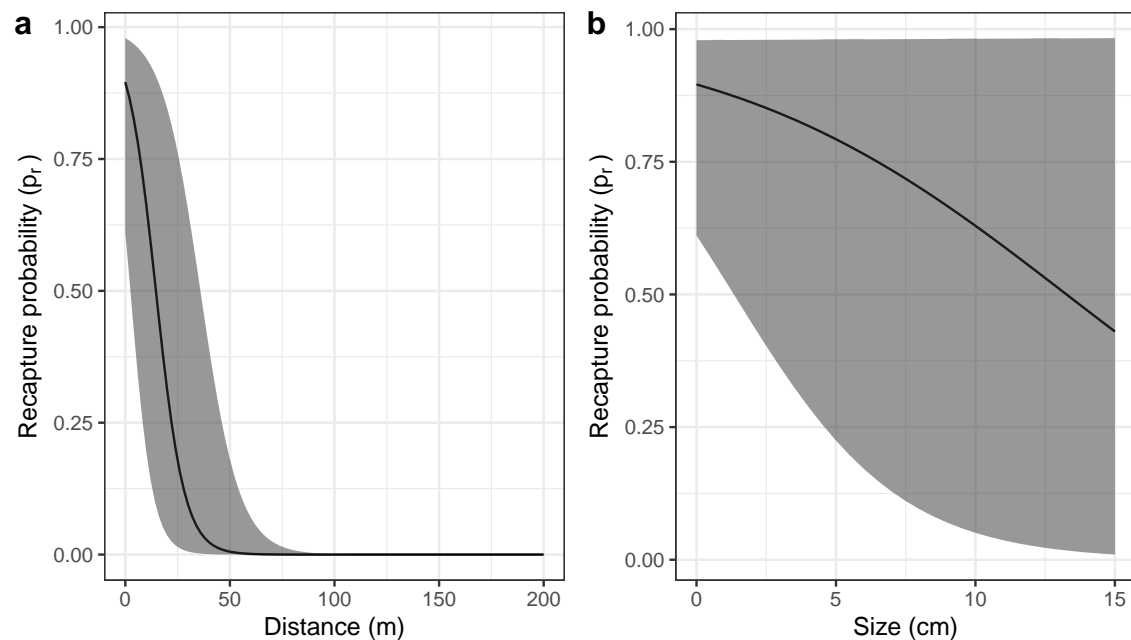


Figure D.6: Effects of a) minimum distance between divers and the anemone where the fish was first caught and b) fish size on recapture probability p_r , estimated along with survival in a mark-recapture analysis (Appendix Methods A.3 and Appendix Results B.4).

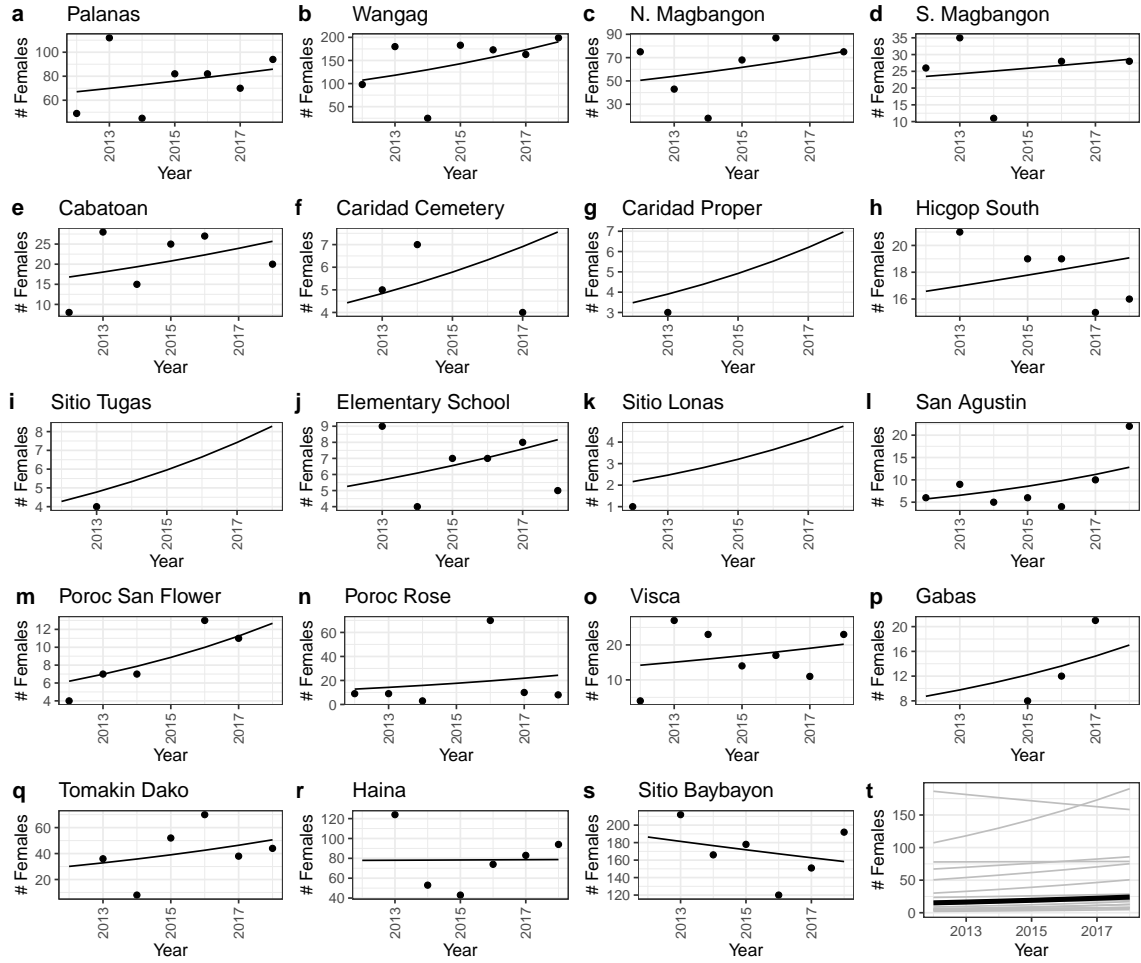


Figure D.7: Scaled number of females captured ($F_{c_i,t}$, black dots) and abundance trends (black lines) by patch from a mixed effects model with patch as a random effect.

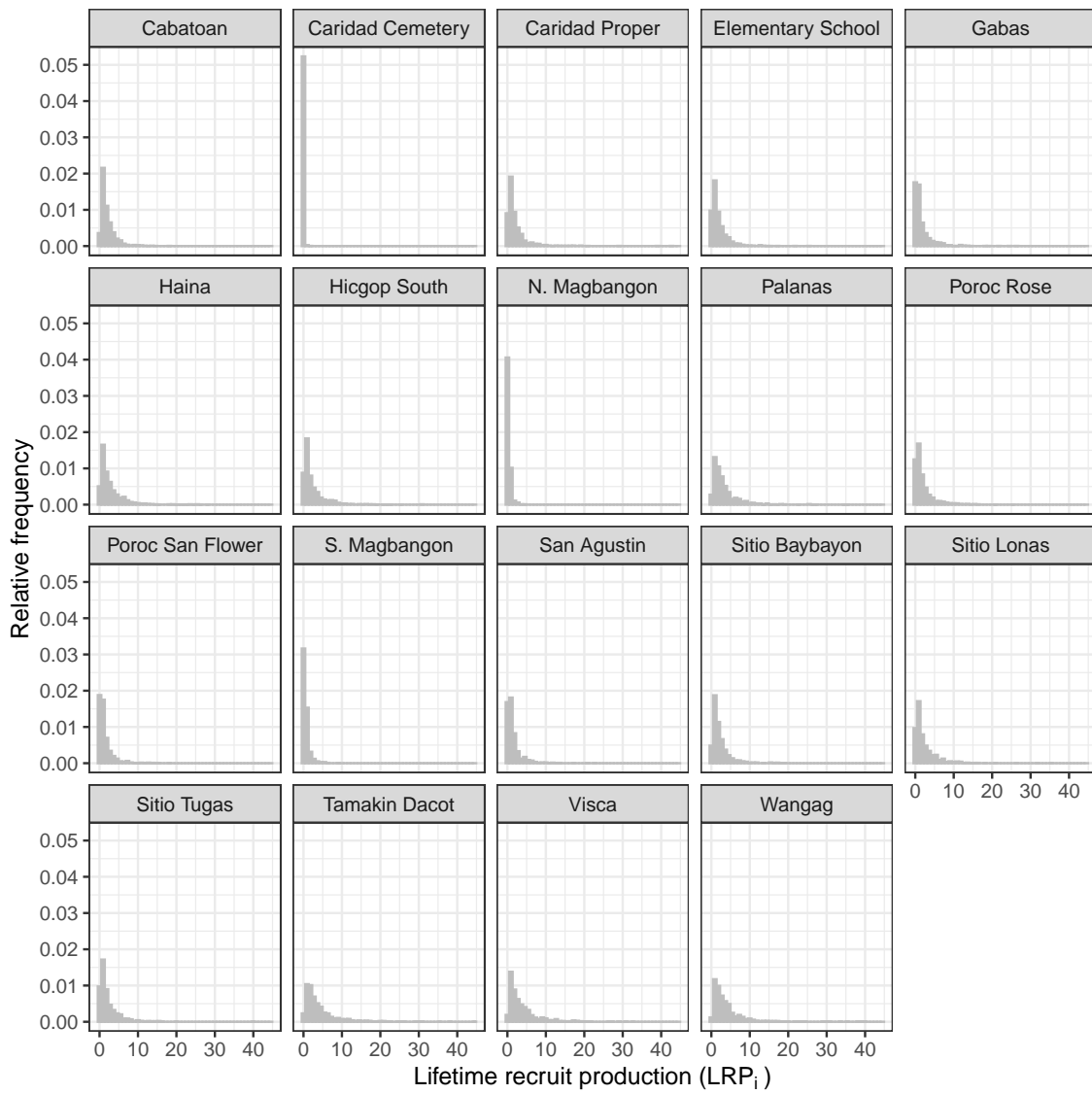


Figure D.8: Patch-specific lifetime recruit production (LRP_i) estimates.

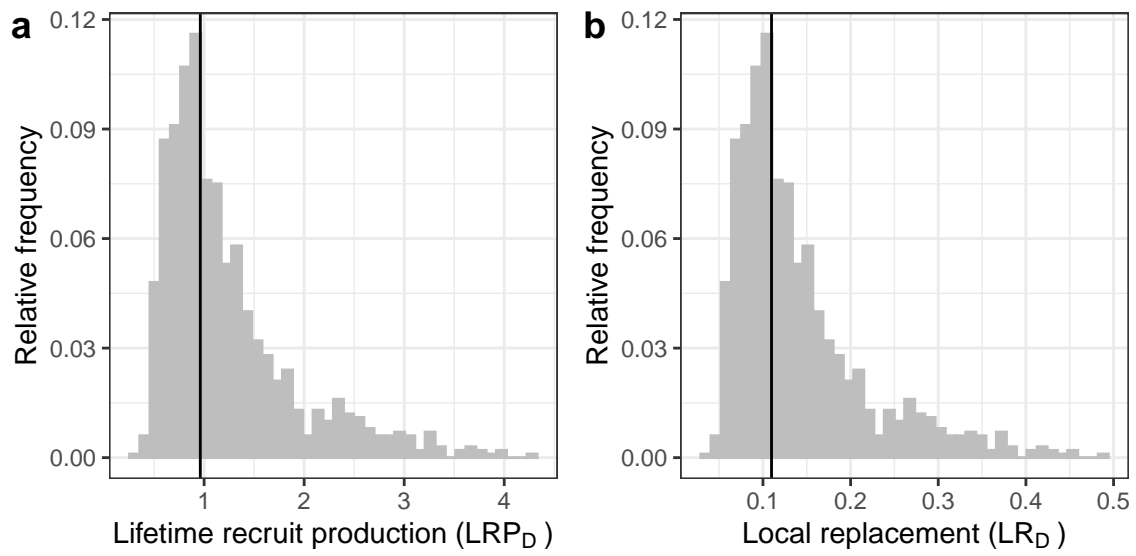


Figure D.9: Estimates of a) LRP averaged across patches, and b) local replacement without compensating for density dependence in early life stages in our data, showing the best estimate (black solid line) and range of estimates considering uncertainty (grey). These estimates compare to those in Fig. 4b and c, where we compensated for additional mortality in early life due to density dependence.

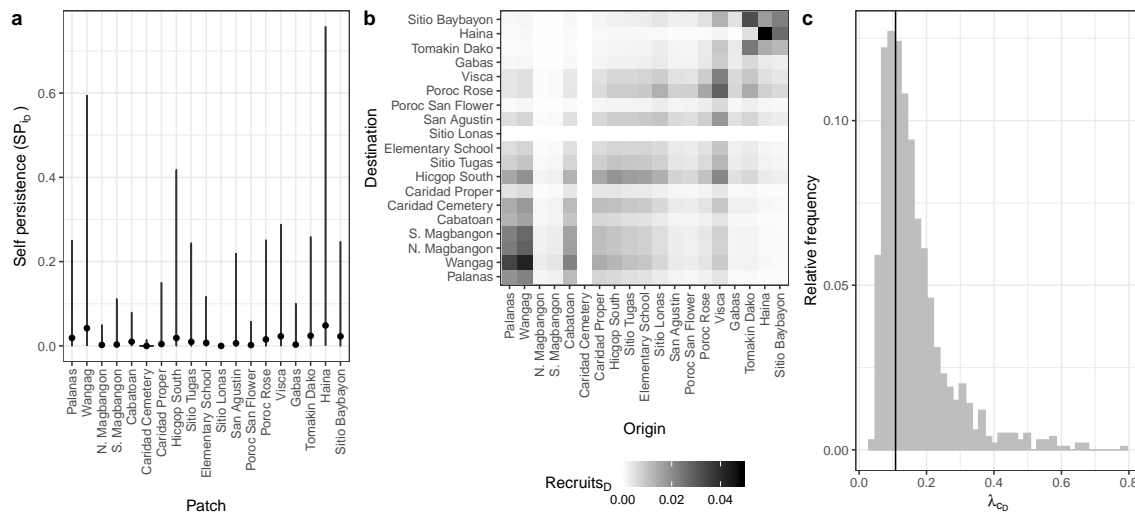


Figure D.10: Values of a) self-persistence (SP_{iD}), b) realized connectivity among patches ($C_{i,jD}$), and c) network persistence (λ_{cD}) without compensation for density-dependence in early life stages in our data. For self-persistence (a) and network persistence (c), the best estimate is shown with in black (point for (a), line for (c)) and the range of estimates considering uncertainty is shown in grey. These estimates compare to those in Fig. 5 where we compensated for density dependence in early life stages.

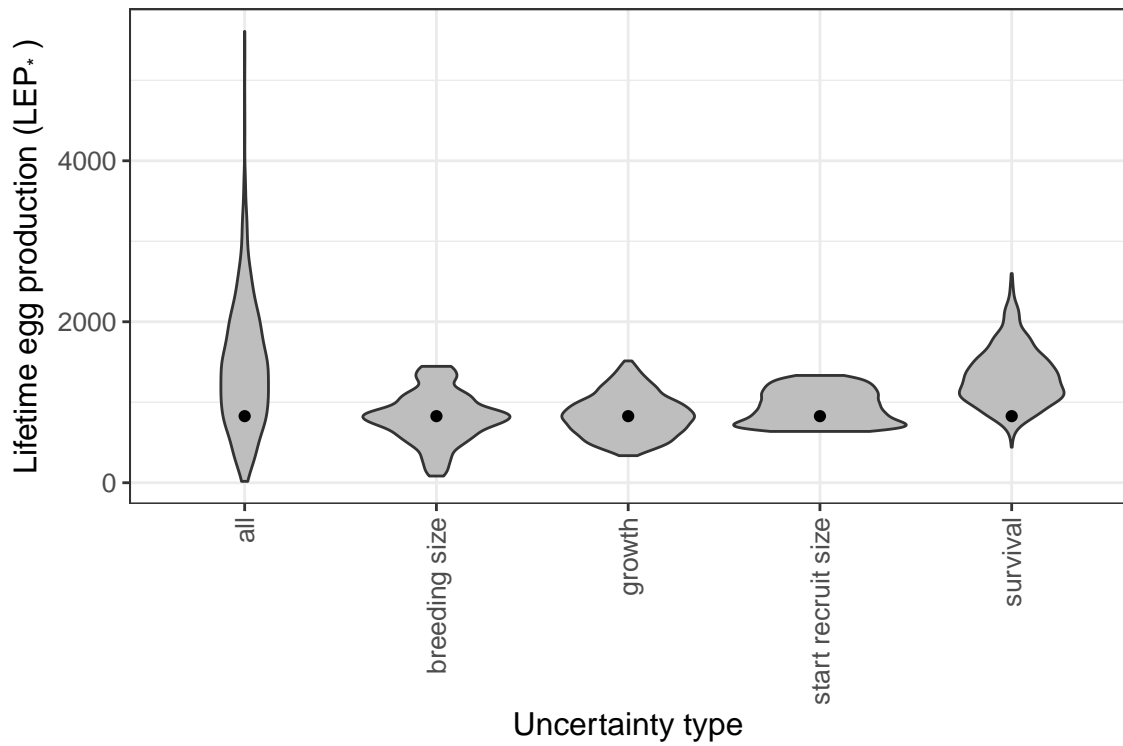


Figure D.11: The contribution of different sources of uncertainty in LEP averaged across patches (LEP_*). We calculated the metrics using best estimates for all inputs except the one shown and show the results as violin plots, which show vertical probability densities of the metrics across a range of values.

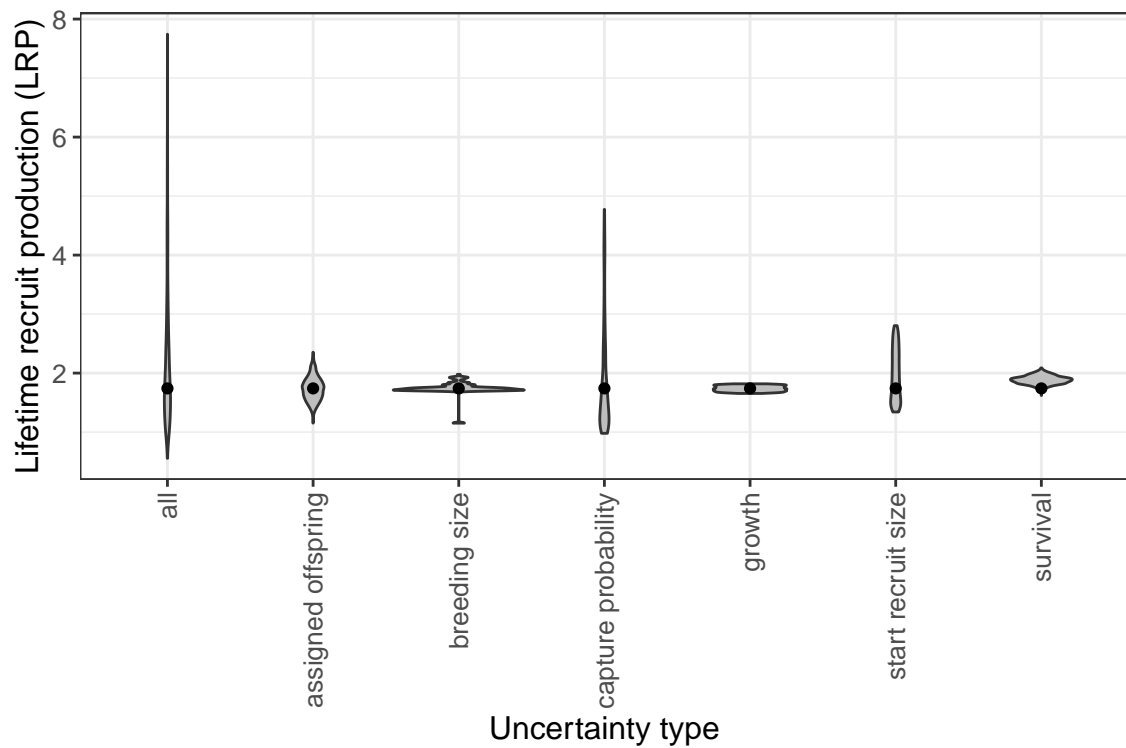


Figure D.12: The contribution of different sources of uncertainty in LRP averaged across patches. We calculated the metrics using best estimates for all inputs except the one shown and show the results as violin plots, which show vertical probability densities of the metrics across a range of values.

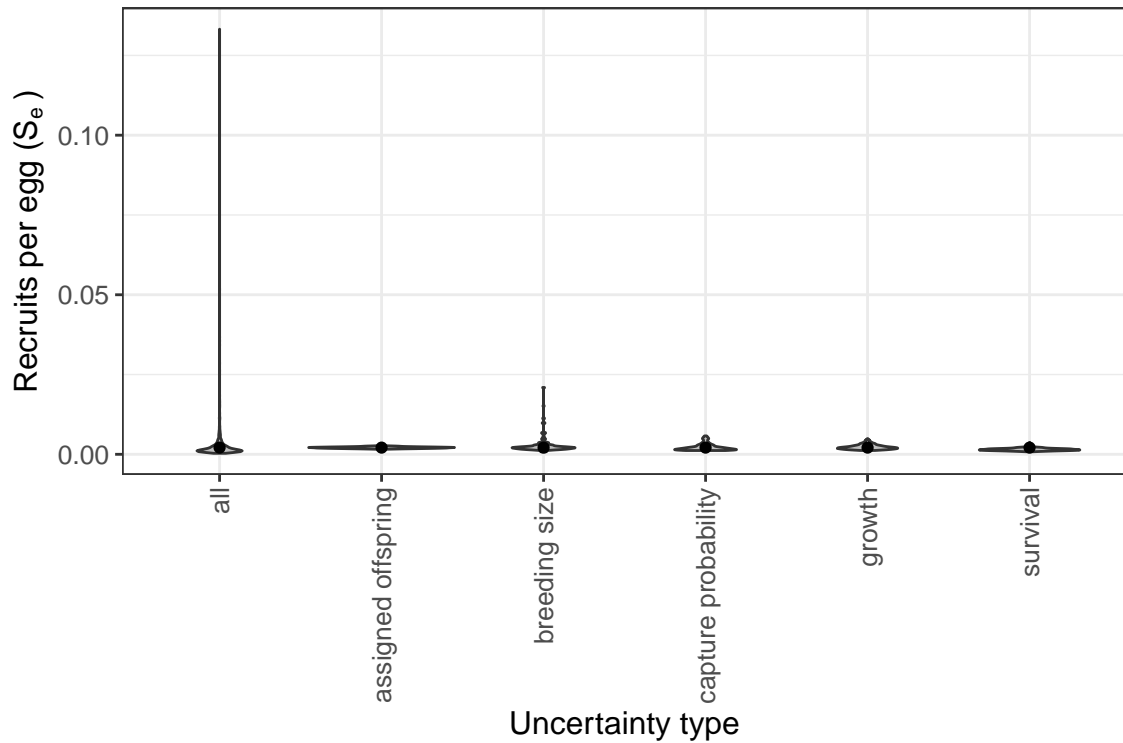


Figure D.13: The contribution of different sources of uncertainty in egg-recruit survival (S_e). We calculated the metrics using best estimates for all inputs except the one shown and show the results as violin plots, which show vertical probability densities of the metrics across a range of values.

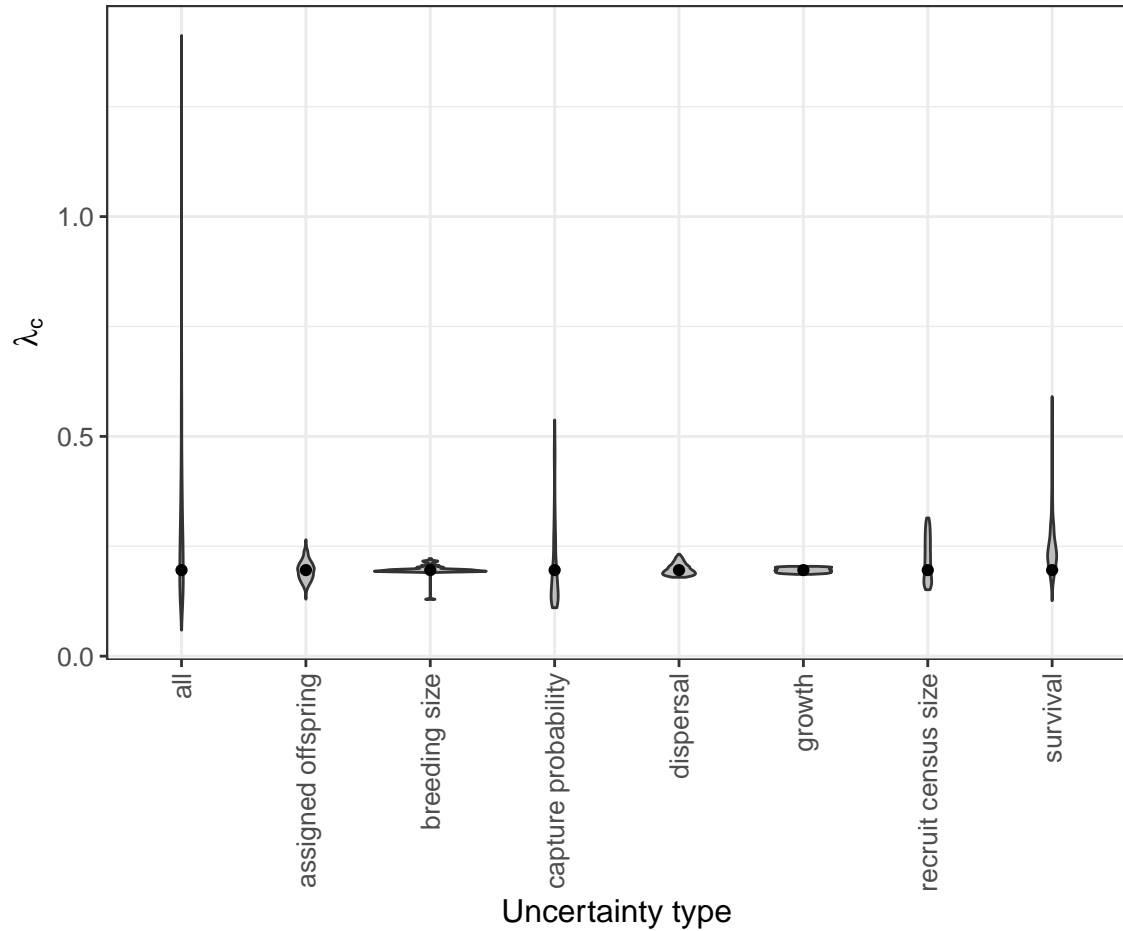


Figure D.14: The contribution of different sources of uncertainty in network persistence (λ_c). We calculated the metrics using best estimates for all inputs except the one shown and show the results as violin plots, which show vertical probability densities of the metrics across a range of values.

References

- Almany, G. R., S. Planes, S. R. Thorrold, M. L. Berumen, M. Bode, P. Saenz-Agudelo, et al. (2017). Larval fish dispersal in a coral-reef seascape. *Nature Ecology & Evolution*, 1:0148.
- Almany, G. R., M. L. Berumen, S. R. Thorrold, S. Planes, and G. P. Jones. (2007). Local replenishment of coral reef fish populations in a marine reserve. *Science*, 316 (5825):742–744.
- Arvedlund, M., M. I. McCormick, D. G. Fautin, and M. Bildsøe. (1999). Host recognition and possible imprinting in the anemonefish *Amphiprion melanopus* (Pisces: Pomacentridae). *Marine Ecology Progress Series*, 188:207–218.
- Bates, D., M. Mächler, B. Bolker, and S. Walker. (2015). Fitting linear mixed-effects models using lme4. *Journal of Statistical Software*, 67(1):1–48.
- Bellwood, D. R. and R. Fisher. (2001). Relative swimming speeds in reef fish larvae. *Marine Ecology Progress Series*, 211:299–303.
- Bode, M., D. H. Williamson, H. B. Harrison, N. Outram, and G. P. Jones. (2018). Estimating dispersal kernels using genetic parentage data. *Methods in Ecology and Evolution*, 9(3):490–501.
- Botsford, L. W., A. Hastings, and S. D. Gaines. (2001). Dependence of sustainability on the configuration of marine reserves and larval dispersal distance. *Ecology Letters*, 4:144–150.

Botsford, L. W., J. W. White, and A. Hastings. (2019). *Population Dynamics for Conservation*. Oxford University Press.

Brewer, C. A. (2020). <http://www.ColorBrewer.org>, accessed 18 August 2020.

Burgess, S. C., K. J. Nickols, C. D. Griesemer, L. A. K. Barnett, A. G. Dedrick, E. V. Satterthwaite, et al. (2014). Beyond connectivity: how empirical methods can quantify population persistence to improve marine protected-area design. *Ecological Applications*, 24(2):257–270.

Buston, P. (2003a). Forcible eviction and prevention of recruitment in the clown anemonefish. *Behavioral Ecology*, 14(4):576–582.

Buston, P. (2003b). Social hierarchies: size and growth modification in clownfish. *Nature*, 424(6945):145–146.

Buston, P. M. and C. C. D'Aloia. (2013). Marine ecology: reaping the benefits of local dispersal. *Current Biology*, 23(9):R351–R353.

Buston, P. M. and J. Elith. (2011). Determinants of reproductive success in dominant pairs of clownfish: a boosted regression tree analysis. *Journal of Animal Ecology*, 80(3):528–538.

Buston, P. M., G. P. Jones, S. Planes, and S. R. Thorrold. (2011). Probability of successful larval dispersal declines fivefold over 1 km in a coral reef fish. *Proceedings of the Royal Society of London B: Biological Sciences*, rspb20112041.

Carson, H. S., G. S. Cook, P. C. López-Duarte, and L. A. Levin. (2011). Evaluating the importance of demographic connectivity in a marine metapopulation. *Ecology*, 92(10):1972–1984.

Catalano, K. A., A. G. Dedrick, M. R. Stuart, J. Purtiz, H. R. Montes, Jr., and M. L. Pinsky. (in review). Quantifying dispersal variability among nearshore marine populations.

Cinner, J. E., C. Huchery, M. A. MacNeil, N. A. J. Graham, T. R. McClanahan, J. Maina, et al. (2016). Bright spots among the worlds coral reefs. *Nature*, 535 (7612):416–419.

Coleman, M. A., P. Cetina-Heredia, M. Roughan, M. Feng, E. Sebille, and B. P. Kelaher. (2017). Anticipating changes to future connectivity within a network of marine protected areas. *Global Change Biology*, 23(9):3533–3542.

D'Aloia, C. C., S. M. Bogdanowicz, J. E. Majoris, R. G. Harrison, and P. M. Buston. (2013). Self-recruitment in a Caribbean reef fish: a method for approximating dispersal kernels accounting for seascape. *Molecular Ecology*, 22(9):2563–2572.

Elliott, J. K., J.M. Elliott, and R.N. Mariscal. (1995). Host selection, location, and association behaviors of anemonefishes in field settlement experiments. *Marine Biology*, 122(3):377–389.

Ellner, S. P., D. Z. Childs, and M. Rees. (2016). Data-driven modelling of structured populations. *A practical guide to the Integral Projection Model*. Springer.

Fahrig, L. (2001). How much habitat is enough? *Biological Conservation*, 100(1): 65–74.

Fautin, D. G. and G. R. Allen. (1992). Field guide to anemonefishes and their host sea anemones. Western Australian Museum.

Figueira, W. F. (2009). Connectivity or demography: defining sources and sinks in coral reef fish metapopulations. *Ecological Modelling*, 220(8):1126–1137.

Figueira, W. F. and L. B. Crowder. (2006). Defining patch contribution in source-sink metapopulations: the importance of including dispersal and its relevance to marine systems. *Population Ecology*, 48(3):215–224.

Figueira, W. F., S. J. Lyman, L. B. Crowder, and G. Rilov. (2008). Small-scale demographic variability of the bicolor damselfish, *Stegastes partitus*, in the Florida Keys, USA. *Environmental Biology of Fishes*, 81(3):297–311.

Fisher, R. (2005). Swimming speeds of larval coral reef fishes: impacts on self-recruitment and dispersal. *Marine Ecology Progress Series*, 285:223–232.

Fuller, E., E. Brush, and M. L. Pinsky. (2015). The persistence of populations facing climate shifts and harvest. *Ecosphere*, 6(9):1–16.

Hameed, S. O., J. W. White, S. H. Miller, K. J. Nickols, and S. G. Morgan. (2016). Inverse approach to estimating larval dispersal reveals limited population connectivity along 700 km of wave-swept open coast. *Proceedings of the Royal Society B: Biological Sciences*, 283(1833):20160370.

- Hanski, I. (1998). Metapopulation dynamics. *Nature*, 396(6706):41–49.
- Harms, K. E., S. J. Wright, O. Calderón, A. Hernandez, and E. A. Herre. (2000). Pervasive density-dependent recruitment enhances seedling diversity in a tropical forest. *Nature*, 404(6777):493–495.
- Hart, D. R. and A. S. Chute. (2009). Estimating von Bertalanffy growth parameters from growth increment data using a linear mixed-effects model, with an application to the sea scallop *Placopecten magellanicus*. *ICES Journal of Marine Science*, 66 (10):2165–2175.
- Hastings, A. and L. W. Botsford. (2006). Persistence of spatial populations depends on returning home. *Proceedings of the National Academy of Sciences*, 103:6067–6072.
- Hattori, A. and Y. Yanagisawa. (1991). Life-history pathways in relation to gonadal sex differentiation in the anemonefish, *Amphiprion clarkii*, in temperate waters of Japan. *Environmental Biology of Fishes*, 31(2):139–155.
- Hayashi, K., K. Tachihara, and J. D. Reimer. (2019). Low density populations of anemonefish with low replenishment rates on a reef edge with anthropogenic impacts. *Environmental Biology of Fishes*, 102(1):41–54.
- Hijmans, R. J. (2017). *geosphere: Spherical Trigonometry*. R package version 1.5-7.
- Holtswarth, J. N., S. B. San Jose, H. R. Montes Jr., J. W. Morley, and M. L Pin-

- sky. (2017). The reproductive seasonality and fecundity of yellowtail clownfish (*Amphiprion clarkii*) in the Philippines. *Bulletin of Marine Science*, 93.
- Johnson, D. W., M. R. Christie, T. J. Pusack, C. D. Stallings, and M. A. Hixon. (2018). Integrating larval connectivity with local demography reveals regional dynamics of a marine metapopulation. *Ecology*, 99(6):1419–1429.
- Jones, G. P., M. J. Milicich, M. J. Emslie, and C. Lunow. (1999). Self-recruitment in a coral reef fish population. *Nature*, 402(6763):802–804.
- Kaplan, D. M., L. W. Botsford, M. R. O’Farrell, S. D. Gaines, and S. Jorgensen. (2009). Model-based assessment of persistence in proposed marine protected area designs. *Ecological Applications*, 19(2):433–448.
- Kritzer, J. P. and P. F. Sale. (2006). *Marine Metapopulations*. Elsevier Academic Press.
- Laake, J. L. (2013). RMark: An R interface for analysis of capture-recapture data with MARK. R package version 2.2.6.
- Lecchini, D., S. Planes, and R. Galzin. (2005). Experimental assessment of sensory modalities of coral-reef fish larvae in the recognition of their settlement habitat. *Behavioral Ecology and Sociobiology*, 58(1):18–26.
- Moilanen, A., A. T. Smith, and I. Hanski. (1998). Long-term dynamics in a metapopulation of the American pika. *The American Naturalist*, 152(4):530–542.

- Moyer, J. T. (1976). Geographical variation and social dominance in Japanese populations of the anemonefish *Amphiprion clarkii*. *Japanese Journal of Ichthyology*, 23(1):12–22.
- Nowicki, P. and V. Vrabec. (2011). Evidence for positive density-dependent emigration in butterfly metapopulations. *Oecologia*, 167(3):657.
- Nowicki, P., S. Bonelli, F. Barbero, and E. Balletto. (2009). Relative importance of density-dependent regulation and environmental stochasticity for butterfly population dynamics. *Oecologia*, 161(2):227–239.
- Ochi, H. (1989). Mating behavior and sex change of the anemonefish, *Amphiprion clarkii*, in the temperate waters of southern Japan. *Environmental Biology of Fishes*, 26(4):257–275.
- Pinsky, M. L., H. R. Montes Jr, and S. R. Palumbi. (2010). Using isolation by distance and effective density to estimate dispersal scales in anemonefish. *Evolution*, 64(9): 2688–2700.
- Puckett, B. J. and D. B. Eggleston. (2016). Metapopulation dynamics guide marine reserve design: importance of connectivity, demographics, and stock enhancement. *Ecosphere*, 7(6).
- Pulliam, H. R. (1988). Sources, sinks, and population regulation. *The American Naturalist*, 132(5):652–661.
- Rodenhouse, N. L., T. S. Sillett, P. J. Doran, and R. T. Holmes. (2003). Multiple

density-dependence mechanisms regulate a migratory bird population during the breeding season. *Proceedings of the Royal Society of London. Series B: Biological Sciences*, 270(1529):2105–2110.

Sale, P. F., I. Hanski, and J. P. Kritzer. (2006). The merging of metapopulation theory and marine ecology: establishing the historical context. In *Marine Metapopulations*, pp. 3–28. Elsevier.

Salles, O. C., G. R. Almany, M. L. Berumen, G. P. Jones, P. Saenz-Agudelo, M. Srinivasan, et al. (2020). Strong habitat and weak genetic effects shape the lifetime reproductive success in a wild clownfish population. *Ecology Letters*, 23(2):265–273.

Salles, O. C., J. A. Maynard, M. Joannides, C. M. Barbu, P. Saenz-Agudelo, G. R. Almany, et al. (2015). Coral reef fish populations can persist without immigration. *Proceedings of the Royal Society B: Biological Sciences*, 282(1819):20151311.

Smedbol, R. K., A. McPherson, M. M. Hansen, and E. Kenchington. (2002). Myths and moderation in marine metapopulations? *Fish and Fisheries*, 3(1):20–35.

Smith, J. N. M. and J. J. Hellmann. (2002). Population persistence in fragmented landscapes. *Trends in Ecology & Evolution*, 17(9):397–399.

Thompson, D. M., J. Kleypas, F. Castruccio, E. N. Curchitser, M. L. Pinsky, B. Jönsson, et al. (2018). Variability in oceanographic barriers to coral larval dispersal: Do currents shape biodiversity? *Progress in Oceanography*, 165:110–122.

- Tolimieri, N. and P. S. Levin. (2005). The roles of fishing and climate in the population dynamics of bocaccio rockfish. *Ecological Applications*, 15(2):458–468.
- Vermeij, M. J. A. and S. A. Sandin. (2008). Density-dependent settlement and mortality structure the earliest life phases of a coral population. *Ecology*, 89(7):1994–2004.
- Warner, R. R. and P. L. Chesson. (1985). Coexistence mediated by recruitment fluctuations: a field guide to the storage effect. *The American Naturalist*, 125(6):769–787.
- Warner, R. R. and T. P. Hughes. (1988). The population dynamics of reef fishes. 6th International Coral Reef Symposium Executive Committee.
- White, J. W. and J. F. Samhouri. (2011). Oceanographic coupling across three trophic levels shapes source–sink dynamics in marine metacommunities. *Oikos*, 120(8):1151–1164.
- White, J. W., M. H. Carr, J. E. Caselle, L. Washburn, C. B. Woodson, S. R. Palumbi, et al. (2019). Connectivity, dispersal, and recruitment: Connecting benthic communities and the coastal ocean. *Oceanography*, 32(3):50–59.
- White, J. W., L. W. Botsford, A. Hastings, and J. L. Largier. (2010). Population persistence in marine reserve networks: incorporating spatial heterogeneities in larval dispersal. *Marine Ecology Progress Series*, 398:49–67.